Receptors for Hyaluronic acid and Poliovirus:

Expression and Role in Glioma Invasion

Zaynah Maherally

This thesis is submitted in partial fulfilment of the requirements for the award of Doctor of Philosophy of the University of Portsmouth

January 2011

DECLARATION

Whilst registered as a candidate for the above degree, I have not been registered for any other research award. The results and conclusions embodied in this thesis are the work of the named candidate and have not submitted for any other academic award.

TABLE OF CONTENT

ABSTRACT

Tumour invasion is the key element in the high rate of mortality and morbidity in glioma patients. The increased levels of expression of the cell surface adhesion molecules CD44/CD155 on neoplastic cells have been highlighted in several studies; both playing a role in glioma invasion. CD44; originally described as the lymphocyte homing receptor, is a cell adhesion molecule with two isoforms with respective molecular weights of 80-90 kDa and 150kDa. CD44 mediates glioma cell adhesion and invasion through its interaction with hyaluronic acid (HA). CD155, also known as the poliovirus receptor, is a transmembrane glycoprotein, the ectodomain of which mediates cell attachment to the extracellular matrix component, vitronectin. Within the scope of this thesis, an up-regulation of CD44 and CD155 has been demonstrated on established cell line (SNB-19) and early passage cultures of biopsy-derived glioma (UPAB and UPMC) using immunocytochemistry and flow cytometry. TIRF microscopy has revealed that CD44 and CD155 are located in close proximity in all the GBM cells studied. CD44 antibody blocking and gene silencing resulted in a higher level of inhibition of invasion than that for CD155 when assessed using the Transwell assay. Interference with combined CD44/CD155 resulted in 86% inhibition of invasion in post-transfected cells. Live cell imaging showed reduced speed of motility and distance travelled in knocked-down cells over their controls. Both siRNA CD44 and siRNA CD155 cells were devoid of filopodia and were rounder in morphology compared to wild type cells. The ECM cell adhesion array demonstrated wild type cells adhered most efficiently to laminin whereas siRNA-treated cells showed decreased adhesive potential on most of the ECMs used. The BrdU cell proliferation assay showed a higher proliferative rate of siRNA CD44 and siRNA

CD155 treated cells was achieved and this was inversely correlated with the reduced invasion of these cells. Confocal microscopy showed distinct overlapping of CD155 and the integrins (β_1, $\alpha_v\beta_1$ and $\alpha_v\beta_3$) on extending processes of the GBM cells whereas siRNA-transfected cells showed consequent reduction in expression level of the integrins with no specific staining patterns. RHO GTPases assay showed reduced expression levels of Cdc42, Rac1/2/3 and RhoA in siRNA transfected CD44 and CD155 cells. No change in expression level of RhoC was observed in siRNA CD155 cells compared to the control cells and the expression levels of RhoB were unchanged in both transfected and control cells. Joint CD44/CD155 approaches may merit further study in targeting infiltrating glioma cells in therapeutic protocols.

LIST OF TABLES

LIST OF FIGURES

ABBREVIATIONS

B-BB	Blood Brain Barrier
BLAST	Basic Local Alignment Search Tool
bp	Base pair
BrdU	Bromodeoxyuridine
BSA	Bovine Serum Albumin
CAM	Cell Adhesion Molecules
CNS	Central Nervous System
CSF	Cerebrospinal Fluid
CT	Chemotherapy
DAP3	Death-Associated Protein-3
dH_2O	Deionised water
DMEM	Dulbecco's Modified Eagles Medium
DMSO	Dimethylsulfoxide
DNA	Deoxyribonucleic Acid
ECM	Extracellular Matrix
EDTA	Ethylenediaminetetraacetic Acid
EGFR	Epidermal Growth Factor Receptor
F-Actin	Filamentous Actin
FCS	Foetal Calf Serum
GBM	Glioblastoma Multiforme
HA	Hyaluronic Acid
HASA	Hyaluronic Acid Stimulating Activity
HBSS	Hanks Balanced Salt Solution
HLA	Human Leukocyte Antigen
HRP	Horseradish Peroxide
ICC	Immunocytochemistry
LCM	Laser Capture Microdissection
LOH	Loss of Heterozygosity
MAb	Monoclonal Antibody
MDCK	Madin-Darby Canine Kidney
MDM2	Murine Double Minute 2

MGMT	O^6-Methylguanine-DNA Methyltransferase
MI	Mitotic Index
MMP	Matrix Metalloproteinases
MRI	Magnetic Resonance Imaging
NA	Numerical Aperture
$NaCl_2$	Sodium Chloride
NaOH	Sodium Hydroxide
NCAM	Neural Cell Adhesion Molecules
NICE	National Institute for Health and Clinical Excellence
OD	Optical Density
PBS	Phosphate Buffered Saline
PCNA	Proliferating Cell Nuclear Antigen
PCR	Polymerase Chain Reaction
PDGF	Platelet-Derived Growth Factor
$PDGF_{AB}$	Platelet-Derived Growth Factor-AB
PDT	Population Doubling Time
PFA	Paraformaldehyde
PI	Propidium Iodide
PTEN	Phosphatase and Tensin Homolog
PVDF	Polyvindyldenefluoride
PVR	Poliovirus Receptor
qRT-PCR	Quantitative Reverse Transcriptase-PCR
RHAMM	Receptor for Hyaluronic Acid-Mediated Motility
RNA	Ribonucleic Acid
RNAi	RNA interference
rpm	revolution per minute
RT	Radiotherapy
RT-PCR	Reverse Transcriptase-PCR
SDS-PAGE	Sodium Dodecylsulfate Polyacrylamide Gel Electrophoresis
SFM	Serum Free Medium
siRNA	Small Interfering RNA
TBS	Tris Buffered saline
TBST	Tris-buffered Saline-Tween

TGFβ	Transforming Growth Factor-Beta
TIMP	Tissue Inhibitors of Metalloproteinases
TIRF	Total Internal Reflected Fluorescence
TMB	Tetramethylbenzidine
VEGF	Vascular Endothelial Growth Factor
WHO	World Health Organisation

DISSEMINATION

Conferences/meetings:

- Maherally Z, Whitaker G and Pilkington G J
  Meeting: Institute of Biomedical and Biomolecular sciences (IBBS)
  Location: Portsmouth, UK (2008)
  Poster presentation
  Title: CD155 AND CD44 interaction in spread of intrinsic brain tumours

- Zaynah Maherally, James R Smith and Geoffrey J Pilkington
  Meeting: British Neuro-Oncology Society (BNOS)
  Location: Hull, UK (2009)
  Poster presentation
  Title: Hyaluronic acid (CD44) and Poliovirus Receptor (CD155): Is co-expression indicative of a combined role in modulating glioma invasion?

- Geoffrey J Pilkington and Zaynah Maherally
  Meeting: Joint Meeting of the Society for Neuro-Oncology (SNO) and the American Association of Neurological Surgeons/Congress of Neurological Surgeons (AANS/CNS)
  Location: New Orleans, USA (2009)
  Poster presentation
  Title: CD44 and CD155: Is their co-expression indicative of a combined role in modulating glioma invasion?

- Zaynah Maherally, James R Smith and Geoffrey J Pilkington
  Meeting: SWARM meeting
  Location: Portsmouth, UK (2010)
  Oral presentation
  Title: CD44 and CD155: Expression and in glioma invasion

- Geoffrey J Pilkington, Zaynah Maherally and James R Smith
  Meeting: The 18th International conference on Brain Tumour Research and Therapy
  Location: Germany (2010)
  Poster presentation
  Title: Hyaluronic acid and Poliovirus Receptors in Glioma Invasion

- Zaynah Maherally, James R Smith and Geoffrey J Pilkington
  Meeting: 6th conference on Experimental and Translational Oncology
  Location: Slovenia (2010)
  Poster presentation
  Title: Hyaluronic acid (CD44) and Poliovirus Receptors (CD155): Expression and role in Glioma invasion

- Z Maherally, J R Smith and G J Pilkington
  Meeting: British Neuro-Oncology Society (BNOS)
  Location: Glasgow, Scotland (2010)
  Oral presentation
  Title: Hyaluronic acid and Poliovirus Receptors: Is Dual expression indicative of a combined role in modulating Glioma Invasion

- Maherally Z, Smith J R and Pilkington G J
  Meeting: Institute of Biomedical and Biomolecular sciences (IBBS)
  Location: Portsmouth, UK (2010)
  Oral presentation
  Title: CD155 AND CD44 in glioma invasion

- Zaynah Maherally and Geoffrey J Pilkington
  Meeting: Axon-Glial interactions in the CNS
  Location: Portsmouth, UK (2010)
  Poster presentation
  Title: A functional study of CD44 and CD155 in Glioma invasion

Publications:

1. Fixative Toxicity in immunohistochemistry: using zinc chloride in place of mercuric chloride.
   Authors: SH Chew, J Bott, Z Maherally, K Michalczyk
   Journal: Biotechnic and Histochemistry Journal, Louisville Kentucky USA. 2006
   Status: Submitted

2. Hyaluronic Acid and Poliovirus Receptors: Is co-expression indicative of a combined role in modulating glioma invasion?
   Authors: Maherally Z, Smith J R, Pilkington G J
   Journal: Neuro-oncology. 2009
   Status: Abstract published

3. CD44 and CD155: Is their co-expression indicative of a combined role in modulating glioma invasion?
   Authors: Pilkington G J and Maherally Z
   Journal: Neuro-oncology. 2009. 11:563-699
   Status: Abstract published

4. Hyaluronic acid and Poliovirus receptors: Is Dual expression indicative of a combined role in modulating glioma invasion?
   Authors: Maherally Z, Smith J R, Pilkington G J
   Journal: Neuro-oncology. 2010. Volume 12:1
   Status: Abstract published

5. A functional study of CD44 and CD155 in glioma invasion.
   Authors: Maherally Z and Pilkington G J
   Journal: Journal of Anatomy
   Status: Abstract published

6. CD44 (Hyaluronic acid) and CD155 (Poliovirus Receptors): Role and Expression in Glioma Invasion.
   Authors: Maherally Z, Smith J R, Pilkington G J
   Journal: Neuro-oncology
   Status: *In preparation*

7. Influence of hypoxia on mitochondria morphology and mutations in putative brain tumour stem cells populations.
   Authors: An Q, Maherally Z, Higgins S C, Pilkington G J
   Journal: Cancer Research
   Status: *In preparation*

8. AFM elasticity measurements of high-grade human brain tumour cells.
   Authors: Maherally Z, Dickson L, Smith J R, Pilkington G J
   Journal: Cancer Research
   Status: *In preparation*

ACKNOWLEDGEMENTS

This thesis would not have been possible without the guidance and the help of several individuals who in one way or another contributed and extended their valuable assistance in the preparation until completion of this study.

First and foremost, I am heartily thankful to my supervisor, Professor Geoffrey Pilkington, whose encouragement, supervision and expertise from the preliminary to the concluding level of my thesis enabled me to develop an understanding of the subject.

My utmost gratitude goes to Dr James Smith for his unselfish and unfailing support towards any microscopy work and analysis of data throughout my PhD.

It is a pleasure to pay tribute to all the technical staff of the School of Pharmacy and Biomedical Sciences: Gill Whitaker, Jill Rice and Lowrie Taylor, for their valuable help, kind advice and continuous assistance towards the success of my project.

My heartfelt thanks are also extended to all my colleagues of the Neuro-Oncology Group: Dr Suzanne Birks, Dr Kathryn Fry, Dr Laura Donovan, Dr Samantha Higgins and Dr Qian An, whom have played a key role until completion of my PhD. Their friendliness, untiring support and knowledge shared during these years will be cherished.

My deepest appreciation and special thanks to my brothers: Iqbal and Nabiil, for their love, everlasting faith in my true potential and by simply being there for me throughout my life.

Above all, a sincere thanks to God, the omnipresent for giving me strength to achieve my goals and who continues to make the impossible possible.

DEDICATION

I dedicate this thesis to you

Mum & Dad

whose

unconditional love, trust and presence

have been a source of encouragement and inspiration to me throughout my life and without whom this hard work would not have been possible.

I am forever grateful for all the sacrifices you have made for me.

No words can express my sincere gratitude, love, appreciation and respect to you.

Thank you for everything.

CHAPTER ONE

INTRODUCTION

1.1 Cellular nature of the brain

The two major groups of cells of the adult central nervous system (CNS) are the neurons and glial cells. All neurons share the same basic architecture but can be classified into at least a thousand different types (Kandel, 2000). Glial cells are divided into microglia (phagocytes involved in inflammatory responses (Innamorato, 2009) and macroglia (neuroectodermal in origin), which include astrocytes (Butt, 2005), oligodendrocytes and ependymal cells. Astrocytes are involved in trophic and metabolic support for neurons, neuronal survival and differentiation, neuronal guidance, neurite outgrowth and synaptogenesis. They also participate in brain homeostasis (Araque, 2008). Oligodendrocytes produce myelin which is the lipid-enriched dielectric that forms a membrane around axons essential for salutatory conduction of action potentials in the CNS (Jakovcevski, 2009). Ependymal cells are a specialized epithelial cell type lining the ventricles of the brain and are involved in transport of cerebro spinal fluid and in brain homeostasis (Spassky, 2005).

1.2 Brain tumours and Epidemiology

A brain tumour may be defined as any intracranial mass created by abnormal and uncontrolled cell division, either from the substance of the brain itself or from the surrounding meninges or spread from cancers primarily located in other organs also referred as metastatic tumours. Metastatic tumours within the CNS occur more frequently with increasing age and probably represent the most frequent type of brain tumour in the elderly (Smith and Ironside, 2007). Tumours of the central nervous system (CNS) are the

second most common form of cancer in children and the sixth commonest in adults. Of these, gliomas are the most common CNS tumours in man (Smith and Ironside, 2007). Gliomas account for more than 70% of all brain tumours and of these glioblastomas (GBMs) are both most frequent and most malignant. Recent statistics published by the Office for National Statistics indicate that of the 245,300 new cases of cancer registered in the UK in 2007, 3728 were malignant neoplasms of the brain. It is also reported that around 16,000 new cases of brain tumour (both malignant and benign) are diagnosed each year (Office for National Statistics, Cancer Research UK, Brain Tumour Research, McKinney 2004). The estimated lifetime risk, calculated in 2009 from these statistics, is 1 in 133 for men and 1 in 185 for women. Primary brain tumours are commonly located in the posterior cranial fossa in children and in the anterior two-thirds of the cerebral hemispheres in adults, although they can affect any part of the brain (Pilkington, 2005). Primary brain tumours are bimodal in distribution with peaks of incidence at 5-9 years and 60-75 years (Aldape *et al*., 2003).

1.3 WHO classification of brain tumours

The WHO (World Health Organization) classification is the current international standard for the nomenclature and diagnosis of gliomas and is subsequently classified into four clinical grades, each distinguished by histological characteristics and their presumed cell of origin (Louis *et al*, 2007; Louis, 2008). As the grade number increases, so does the malignancy of the tumour, resulting in the most aggressive, malignant glioblastoma multiforme (GBM). Although several entities have been described in the 4th edition of the

WHO's classification of tumours of the CNS, only GBMs will be considered in the scope of this thesis.

1.4 Gliomas

Glioma is a generic term used to describe primary brain tumours thought to be derived directly from astrocytes, oligodendrocytes or ependymal cells (Sanai *et al*., 2005) or their progenitors. Astrocytomas (WHO grade I to IV) are the most common type of glioma; the major associated tumours being pilocytic astrocytomas (Grade I), diffuse astrocytoma (Grade II), anaplastic astrocytoma (Grade III) and glioblastoma (Grade IV).

1.4.1 Glioblastoma multiforme

The most frequent and biologically aggressive glioma is the glioblastoma multiforme (GBM) (WHO grade IV) (Perry, 2008). Their histopathological features include nuclear atypia, cellular pleomorphism, mitotic activity, vascular thrombosis, microvascular proliferation and necrosis. GBMs primarily affect adults, with a peak incidence ranging between 45 and 75 years (Neal *et al*., 2003) and are preferentially located within the cerebral hemispheres. Most GBMs arise rapidly *de novo*, with no previous lesions and are termed primary GBM. GBMs that arise from diffuse astrocytoma (grade II) or anaplastic astrocytomas (grade III) are termed secondary GBMs. Glioblastoma multiforme (GBM) is the most common astrocytic glioma and can arise with no prior neoplastic disease (Behin *et al*., 2003) or can progress from lower grade gliomas (Dai and Holland, 2001). Moreover,

the time to progression from diffuse astrocytoma (grade II) to GBM varies considerably from less than a year to more than 10 years (Louise *et al*., 2007). The dismal prognosis for glioblastoma patients is due to the invasive nature of the tumour which results in complete resection by surgery and, despite progress in radio/chemotherapy, less than half of patients survive more than a year. Primary GBMs are genetically characterized by LOH 10q, EFGR amplification, $p16^{INK4A}$ deletion which is associated with the retinoblastoma tumour suppressor gene (RB1) (Valle- Folgueral *et al*., 2008) which controls progression through G_1 to S phase of the cell cycle and finally PTEN mutations (Ohgaki and Kleihues, 2007). Despite the short duration of symptoms in many cases of GBM the lesions are often surprisingly large at the time of presentation. The lesion is usually unilateral but those in the brain stem and *corpus callosum* can be bilaterally symmetrical. Infiltrative spread is a hallmark feature of all diffuse astrocytic tumours, however, GBMs are well known for rapid invasion of neighbouring brain structures. A very common feature is extension of the tumour through the *corpus callosum* into the contralateral hemisphere, creating the image of a bilateral, symmetrical lesion referred to as the 'butterfly glioma' (Louis, 2008). As the term glioblastoma 'multiforme' suggests, the histopathology of this tumour varies greatly. While some lesions show a high degree of cellular and nuclear polymorphism with numerous multinucleate giant cells, others are highly cellular (Louis *et al*., 2007).

1.5 Biological features of gliomas

1.5.1 Proliferation

A key element in tumour growth and progression is cellular proliferation and the rate of cell growth correlates closely with prognosis. Cycle dependent chemotherapy is directed at cells which are undergoing mitosis and since mitotic figures are correlated with malignancy, it is therefore important to know what percentage of cells is proliferating.

The mitotic index (MI) is a ratio of cells in mitosis to those which are not. The MI ratio is used when grading tumours. A positive correlation has been found between an increase in mitotic figures and malignancy.

Immunohistochemical cell proliferation markers such as proliferating cell nuclear antigen (PCNA): a co-factor of DNA polymerase-δ which facilitates and controls DNA replication, is involved in the repair of DNA damage, chromatin structure maintenance, chromosome segregation and cell-cycle progression (Stoimenov, 2009), Ki-67 antigen: the Ki-67 protein is present in G1, S, G2 and M phases of the cell cycle, a fraction of which is also detected in quiescent cells (Bullwinkel, 2006) and have been shown to be involved in rRNA synthesis *in vivo* (Rahmanzadeh, 2007), bromodeoxyuridine (BrdU): a thymidine analogue which incorporates into newly synthesised DNA and is also a quantitative measure of DNA synthesis; have come into general use and the marker-positive cell rate is related to histological grading and plays a major role in predicting prognosis (Oda *et al*., 2005).

Many of the genetic aberrations found in gliomas, including p53 mutations, bypass the cell cycle arrest signals and block the natural apoptotic pathways, resulting in neoplastic cells proliferating uncontrollably and continuously (Merzak and Pilkington, 1997).

1.5.2 Cellular Heterogeneity

Clinical management of gliomas currently relies heavily on accurate histopathological diagnosis of grade and subtype for provision of appropriate therapy to individual patients (Walker *et al*., 2003).

The morphological heterogeneity of GBMs has been described since 1865. Genotypically, gliomas and cultured glioma cells have been demonstrated to differ within and among individuals, according to chromosome number, marker chromosomes and DNA content. Phenotypically, cultured glioma cells differ in morphology, growth properties, antigenic expression, tumourgenicity in nude mice, and in response to both radiotherapy and chemotherapeutic agents. The existence of this inherent complex antigenic heterogeneity requires the design of multi-modality therapeutic regimes for each individual patient and tumour (Wikstrand *et al*., 1983). Cultured glioma cells, at least during the early passage retain the cellular heterogeneity seen in histological sections taken at the time of surgery but this is generally lost with overpassaging (Pilkington, 1992) which emphasizes the need to use low passage primary glioma cultures.

Anaplastic changes in gliomas can be diffuse or it may be possible to distinguish areas with low and high grade histological features that may be indicative of progression in some parts of the tumour to a higher grade. Many gliomas show mixed histology with features of more than one histological subtype present within the same tumour sample or in sample obtained from the same patient obtained at different times (Walker *et al*, 2003). Tumour heterogeneity has important morphological, molecular and clinical implications. The knowledge of oncogenical alteractions involved in each tumour can be important to

correlate the morphological features, the genetic background, the prognosis and the clinical response to therapy with anti-cancer agents. Based on the molecular background of the tumour there are new cancer gene therapy protocols such as inhibitors of tyrosine kinase for the PDGF receptor in gliomas (Lleonart *et al*., 2000).

1.5.3 Angiogenesis

Angiogenesis which is the generation of new capillary blood vessels is a characteristic of GBM and is an essential component of many physiological and pathological conditions including growth and metastasis of primary tumours. Solid tumours require angiogenesis to spread larger than a few mm^3 and GBMs are known to be one of the most highly vascularised of all human tumours (Merzak and Pilkington, 1997). It has however, been demonstrated that the rapid growth of GBM results in focal ischaemia and hypoxia, which in turn results in angiogenesis mediated by vascular endothelial growth factor (VEGF) (Giese *et al*., 2003). It has been shown that VEGF and PDGF are greatly overexpressed by tumour cells in human GBM (Nister *et al*., 1988, 1991; Westermark *et al*., 1995). Tumours are also able to target and use pre-existing host vessels by induction of angiopoietin-2 expression by host endothelial cells, thus resulting in the regression of pre-existing vessels, tumour necrosis and subsequent onset of hypoxia induced VEGF-mediated angiogenesis (Zagzag *et al*., 2000).

1.5.4 Invasion

Brain tumours may be primary (intrinsic) or secondary (extrinsic), when cells leave a primary somatic cancer, intravasate into the bloodstream, arrest at a distant organ and eventually develop into gross lesions at the secondary site including the CNS (Mendoza, 2009). The brain is in fact a major site for growth of secondary cancers, with 25% of malignant tumours showing involvement in the brain (Merzak and Pilkington, 1997). Secondary lesions such as these are generally well circumscribed whereas primary brain tumours show marked dissemination at the brain/ tumour interface with poor definition of the tumour edge. This is due to neoplastic cells migrating several millimeters and sometimes even centimeters away from the main tumour mass (Pilkington, 1997 and Bolteus *et al*., 2001). As mentioned previously, there is a preferential invasion of glioma cells along white matter tracts, leading for example to the formation of 'butterfly' lesions, while other gliomas remain confined to the white matter, stopping abruptly at the grey-white matter junction. Other migratory patterns include preferential growth around neurons in the grey matter, perivascular growth and subpial spread (Pilkington, 1994). These typical behaviours imply that glioma cells have either a tropism for particular sites or a restricted ability to invade in the potential regions between specific cell combinations (Louis, 2008). These motile cells termed 'guerilla' cells give rise to recurrent tumours, following surgical and adjuvant chemo and radiotherapeutic intervention (Pilkington, 1997). The ability of glioma cells to invade the surrounding brain tissue prevents gliomas from complete surgical resection and subsequently successful therapy. It has been demonstrated that during this invasive procedure cells transiently arrest from the cell cycle (Pilkington, 1994), therefore leaving them refractory to radiotherapy and the response to

chemotherapy is likely to be poor (Bolteus *et al*., 2001). The mechanisms of invasion, which include complex, interacting processes between cell adhesion molecules, remodeling of the extracellular matrix (ECM) (Rauch, 2004), matrix metalloproteases (MMPs), cytosketon elements (Maidment, 1997), gangliosides, growth factors (Finn *et al*., 1997) and cytokines (Pilkington, 1997), was first described by Liotta (1986) and is still in use to design current models of invasion. Other components which have been associated to invasion include Tenascin C, integrins, cadherins, NCAM and Connexin 43 (Demuth and Berens, 2004).

The invading neoplastic glia are protected from cytotoxic drugs by invading into areas of the brain protected by an intact blood brain barrier (B-BB). Chemotherapeutic agents can infiltrate the main tumour mass where B-BB is compromised but are prevented from reaching the invading cell population (Bolteus *et al*., 2001). Drug delivery to the brain is hampered by a major obstacle in the blood brain barrier and many new approaches to circumvent this have been suggested. These approaches either serve to increase drug delivery of intravascularly administered drugs by manipulating either the drugs or the capillary permeability or to increase drug delivery by local administration (Groothuis, 2000). Further as stipulated by the 'go-or-grow hypothesis' (Bolteus *et al*. 2001), that is, cells either move (invade) or divide, and not both so this transient arrest from the cell cycle means that radiotherapy (and some cell cycle specific anti-tumour drugs) will not work on migratory cell populations.

The invasive phenotype of low and high grade tumours is acquired early on in tumourgenesis (Louis, 2008). Despite the migratory behaviour and invasiveness of primary brain tumours, they rarely metastasize to distant organs (Subramanian, 2002). Pilkington

(1997) explained the above statement by suggesting that; 1) time- gliomas are fatal even before metastases become detectable; 2) immunity-detection and eradication by patient's own immune system; 3) seed-soil hypothesis- whereby glioma cells are unable to grow in different microenvironment; 4) the B-BB may prevent neoplastic glia from leaving the brain and entering the circulatory system and 5) neoplastic glia failing to express the required cell adhesion molecules to adhere to other organ endothelium although the fifth hypothesis is the most likely candidate. Martin *et al* (1995) on the other hand reported that CD15; which has been implicated in mediation of adhesion between haemopoietic cells and vascular endothelium, may be involved in a similar adhesive role between neoplastic cells and endothelia during metastasis; are very low or not expressed on human glioma derived cells.

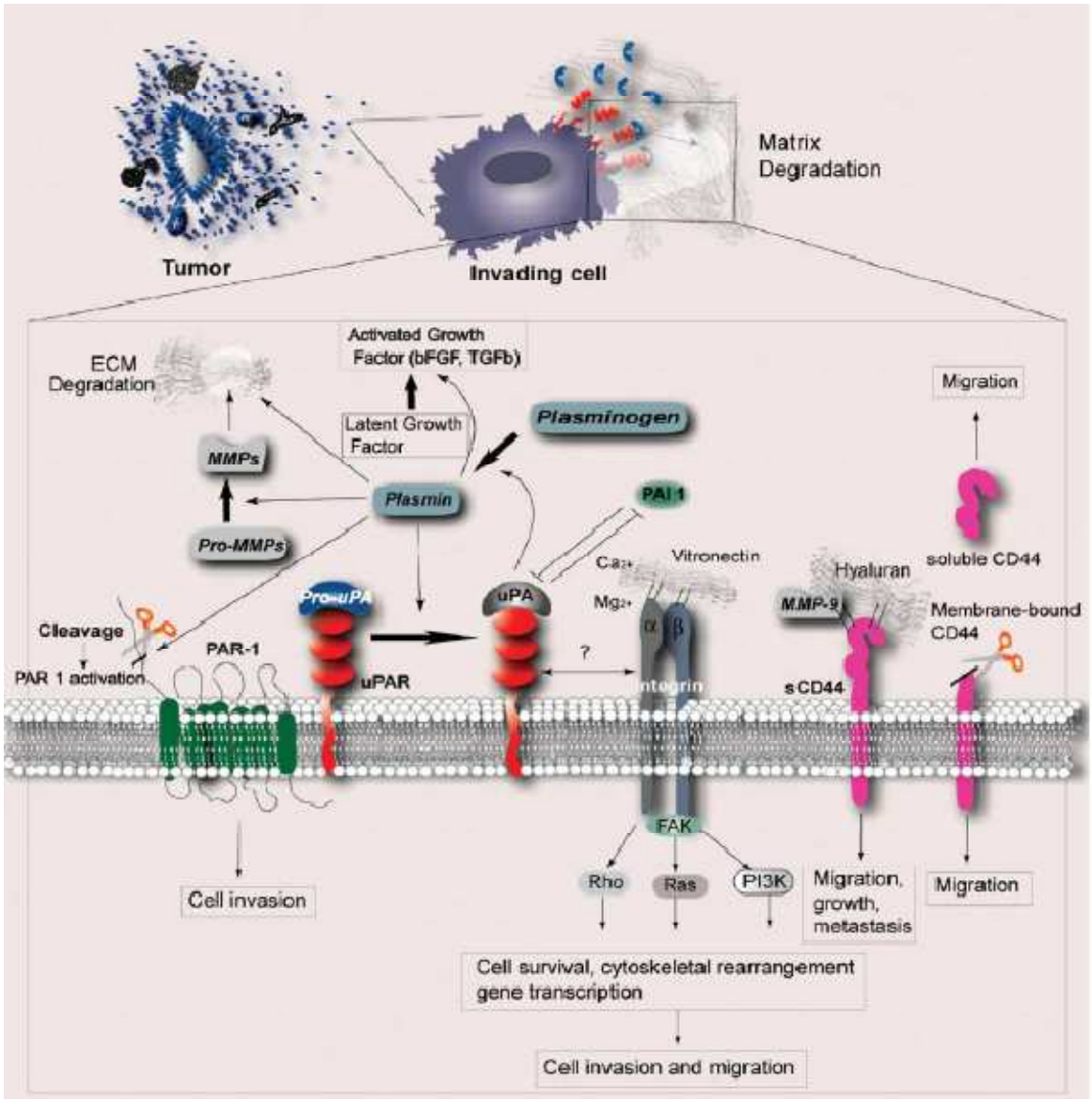

Figure 1: **Schematic representation of the main actors implicated in invasion of brain tissue including urokinase receptor, plasminogen, plasmin, pro-MMPs, PAI-1 (Bellail *et al.*, 2004). Note: CD44 and hyaluronan are included as major players in the invasion cascade; these will be dealt with in more details in the Introduction (section 1.9)**

1.5.4.1 The Extracellular matrix

The ECM affects various functions and processes within the brain. During brain development, the ECM modulates the migration of glial and neuronal precursor cells, synapse formation and cell proliferation.

In primary brain tumour, the ECM is aberrantly over-expressed, often giving rise to bizarre configurations and undergoes considerable remodeling (Pilkington, 1996). Such changes may exert a major influence on brain tumour growth, proliferation and invasion via multiple mechanisms (Bellail *et al*., 2004).

Neural ECM consists of a variety of collagen superfamily molecules and non-collagenous matrix molecules, including hyaluronan, proteoglycans and glycoproteins (Wu, 2005). ECM consists primarily of proteoglycans-lecticans and two ECM components: Tenascin and hyaluronic acid (Ruoslahti, 1996). These are then directly associated with integrins on the cell surface (Viapiano, 2008). ECM is central to the migratory and invasive behaviour of glioma cells mediated through integrins associations with ECM (Luwor, 2008). Brain tumours have shown that with autocrine and paracrine stimulation, both normal and neoplastic cells are capable of producing and secreting ECM components, such as laminin, HA and tenascin-C (Bolteus, 2001) to provide a permissive substrate for invasion. HA is frequently increased in malignant tumours containing higher amounts than in normal brain tissue (Park, 2008) while fibronectin and nonfibrillar collagens (Viapiano, 2006; Viapiano, 2008) and laminins (Sim, 2009) have both been demonstrated to be produced by neoplastic glia.

Glial limitans externa	Collagen (I, III, IV) Fibronectin Laminin Heparin sulphate
Vascular basement membrane	Collagen (IV, V) Laminin Heparan sulphate Proteoglycans Vitronectin Fibronectin
Brain parenchyma	Hyaluronic acid Dermatan sulphate Chrondroitin sulphate Hyaluronectin Tenascin

Table 1: Regional distributions of components of extracellular matrix in the brain (Adapted from: Rao, 2003)

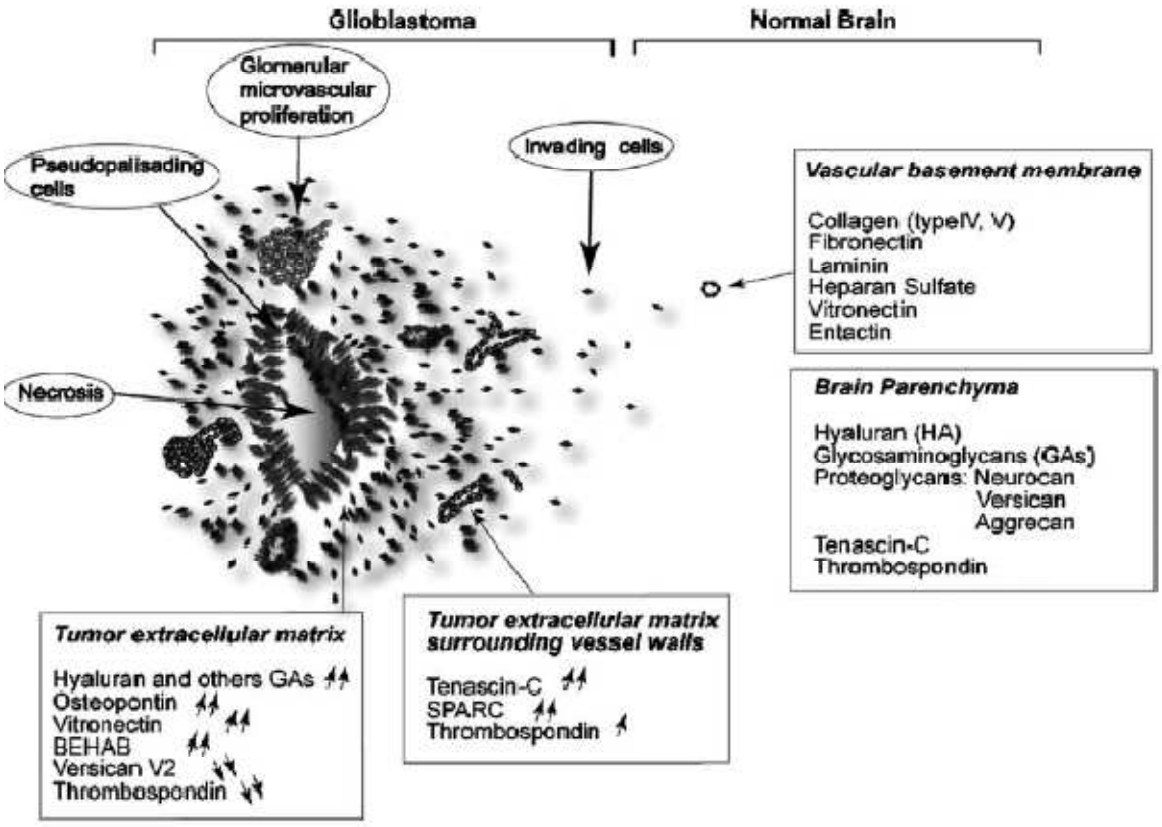

Figure 2: Schematic representation of the heterogeneity and micro regional distribution of the various matrix proteins involved in normal brain and glial tumours (Bellail *et al*., 2004)

1.5.4.2 Matrix Metalloproteases

In vitro and *in vivo* evidence have shown that the expression of specific extracellular matrix proteases stimulates invasive behaviour in gliomas. These include the matrix metalloproteinases (MMPs), the urokinase-dependent plasminogen activating cascade and cathepsin B (Hughes *et al*., 1998).

Matrix metalloproteinases (MMPs) are a family of zinc-dependent endopeptidases (Kahari*et al*., 1997; Shapiro, 1998; Woessner, 1998) subclassified according to their substrate specificity and structures (Westermarck and Kahari, 1999). They include membrane-type MMPs, collagenases, gelatinases and stromelysins (Rao, 2003; VanMeter *et al*., 2001). MMPs are produced in cells as pro-enzymes and require proteolytic cleavage for activation, for example by serine proteases such as plasmin.

Increased expression of MMPs has been linked with many malignancies and seems to play a pivotal part for tumour invasion and metastasis (Basset *et al*., 1997; Johnsen *et al*., 1998). It has been hypothesized that MMPs play a crucial role in tumour invasion due to the presence of high-level expression of distinct MMPs in invasive malignant tumours (Westermarck and Kahari, 1999). Among MMPs, the gelatinases MMP-2 and MMP-9 have been strongly implicated in glioma invasion and have been observed to be expressed in human glioma cell lines and human astrocytoma specimens (Rao, 1993; Sawaya *et al*., 1996) with degree of expression correlating with tumour grade (Forsyth *et al*., 1999). There is also a high correlation between the expression of MMP-2 and MMP-9 and the ability of glioma cells to invade *in vitro* (Abe *et al*., 1994; Uhm *et al*., 1996). MMPs are produced by glioma cells in small quantities ‘on demand’ to remodel/denature the ECM

substrate which has previously been produced either constitutively by the brain tissue or by the tumour cells themselves in order to provide a base for attachment and permissive substrate for invasion. The sequence of events involves:

a. Lamelipod (invadopod) extension
b. CAM expression
c. ECM secretion (in absence of brain derived ECM, e.g, HA)
d. Adhesion/purchase
e. Contractile force (cytoskeletal re-organisation)
f. Progressive movement
g. Denaturing of ECM by e.g MMPs to break bond
h. Repeat of a-g.

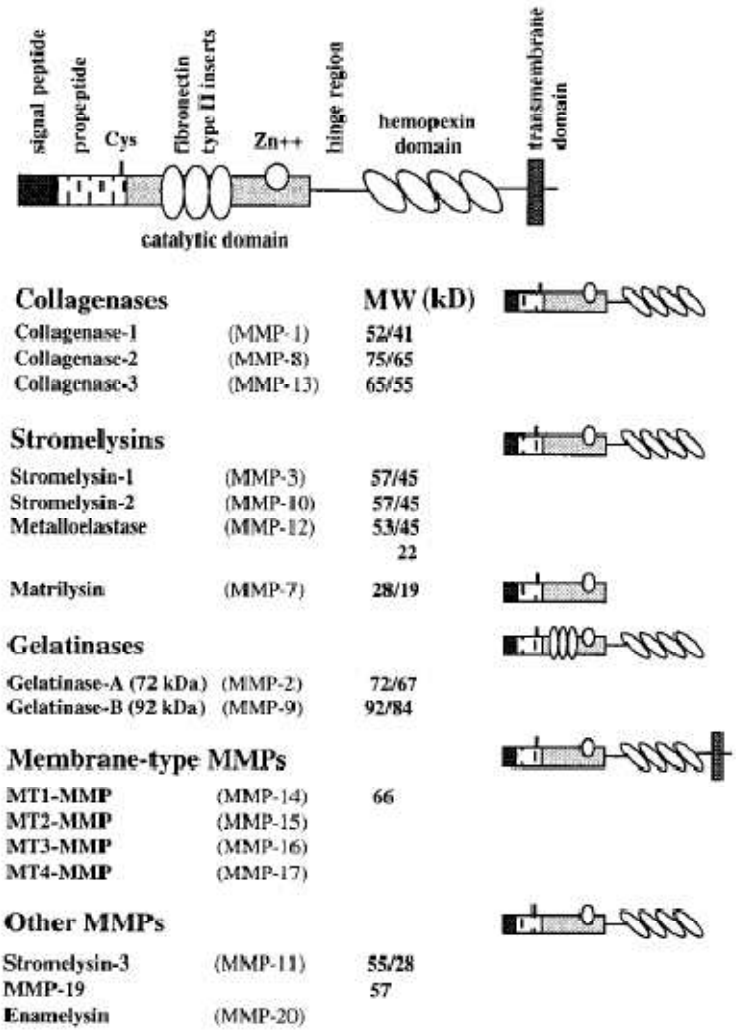

Figure 3: Structure of human matrix metalloproteinases (Adapted from: Kahari *et al*., 1997)

1.5.4.3 Adhesion molecules

Cell adhesion molecules are families of cell surface glycoproteins with large extracellular domains, a membrane spanning region and an intracellular and cytoplasmic functional domain (Goodison *et al*., 1999). They facilitate strong bonding to a specific ligand through a complex process involving the cell 'sensing' the extracellular environment and sending out information to adjacent cells. Cell adhesion molecules (CAMs) such as integrins, cadherins and immunoglobulin proteins (Sloan *et al*., 2004) are involved in cell motility in response to soluble ECM proteins and migration, differentiation, cell signaling and gene transcription (Cheney, 1998). CAM sits at the top of many signaling cascades that regulate actin and microtubule dynamics through Rho GTPases (Bogenrieder and Herlyn, 2003). The 'key' CAMs in glioma invasion are: CD44 and NCAM (Neural Cell Adhesion Molecule).

1.5.4.4 Integrins

Integrins are key molecules on the cell surface which facilitate ECM/CAMs interaction and binding (Uhm *et al*., 1999). They are expressed as cell surface heterodimers consisting of α and β subunits which are non-covalently linked. Currently, 18 different α and 8 different β subunits have been described (Milner and Campbell, 2002). Their mediating role in adhesive events during malignant transformation, tumour growth and progression, invasion and metastasis occurs through provision of a physical transmembrane link between the ECM and the underlying cytoskeletal elements, which results in transduction of bidirectional signals across the cell membrane.

Some integrins bind only one specific ligand while others bind several different ligands and equally, some ECM ligand also bind to multiple integrin (Van der Flier and Sonnenberg, 2001).

β_1 integrin is a 130 kDa transmembrane glycoprotein made up of alpha subunits and form non-covalent complexes with various integrin alpha subunits to form the receptors that bind to specific extracellular matrix proteins and is centrally involved in invasion. β_1 integrin is probably the most common expressed subunit in glioma (Rooprai, 1999).

αv integrin in brain tumours has been linked with glioma invasion either by the fibronectin ligand $\alpha_v\beta_1$ or $\alpha_v\beta_3$ receptor that interacts with vitronectin, tenascin, osteopontin, von willebrand factor or thrombospondin and facilitates extracellular matrix cell adhesion (Bellail *et al*., 2004).

The clustering of integrins on a cell surface leads to the formation of focal contacts. It has also been reported that the interactions between integrins and the extracellular matrix trigger signal transduction pathways and plays a role in regulating gene expression.

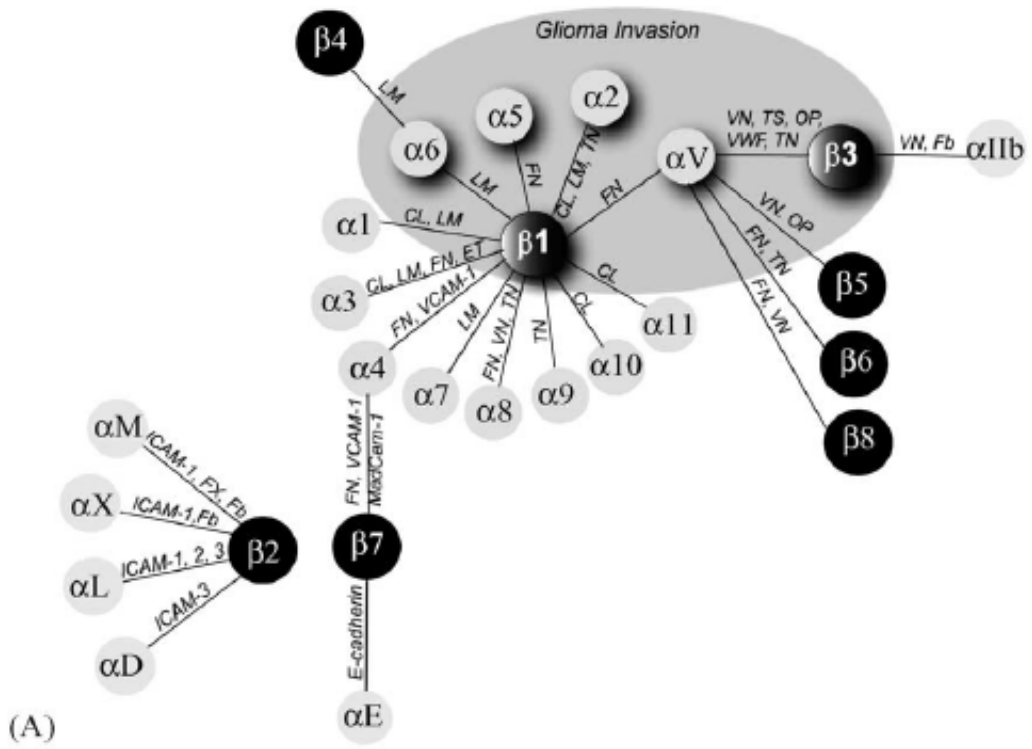

Figure 4: Schematic representation of the integrin subunits and their ligands in glioma invasion (grey shade region) versus normal. Integrins are expressed as heterodimers and fall into three main groups: β_1, β_3 and αv (Bellail *et al*., 2004).

1.6 Proliferation and Invasion

The notion that neoplastic glial cells transiently arrest from the cell cycle during invasion resulted in the theory that glioma cells either 'grow' (proliferate) or 'go' (invade), with these events being mutually exclusive (Bolteus *et al*., 2001). Indeed, many anti-invasion strategies have shown that inhibition of invasion stimulates cell proliferation (Fedotov and Iomin, 2007) and vice versa. Behaviourally, gliomas can be viewed as consisting of two discrete sub-populations of cells, the proliferative cells at the tumour core and the more peripheral cells invading into the brain parenchyma, although these two 'populations' are functionally reversible by modification of cell surface or other molecules required for the

divergent processes of invasion and proliferation. Therefore, the gene expression profile of the tumour core may not depict the genetic profile of the invasive edge. Demuth and Berens (2004) used laser capture microdissection (LCM) of frozen sections from human biopsy samples to isolate cells from the tumour core and the invasive edge and performed cDNA microarrays comparing genes in both subpopulations. This led to the identification of genes differentially expressed in invasive glioma cells and included over expression of P311, Death- associated- protein 3 (DAP3), FN14 and P13-K (Demuth and Berens, 2004). Thier *et al* (2000) evaluated the relationship of proliferation rates using the BrdU labeling index and MMP activity in neuroectodermal tumour cell lines. The expression of some MMPs such as MMP2, MMP9 & MMP14 (MT-MMP) has been found to positively correlate with the degree of malignancy in gliomas. The cell lines with high MMP-2 expression levels recorded low levels of proliferative activity and *vice versa*. The conclusion was that proliferation was inversely correlated to MMP-2 expression in the glioma cells evaluated (Their *et al*., 2000). Research emphasizes that suppression of migration might enhance cell proliferation leading to enhanced tumour cell death by either radiotherapy or chemotherapy.

1.7 Treatment modalities for gliomas

Depending on the type of tumour and its location, the likely course of events will be surgery, radiotherapy (RT) and chemotherapy (CT); however, despite aggressive therapy including combined surgery, radiotherapy and chemotherapy, GBM recurs within 6-12 months (Neider *et al*., 2000). Relapse occurs in approximately 80% of cases usually within

2-3cm of the margin of the original lesion (Neider *et al*., 2000). Currently, the standard treatment modality for high grade malignant glioma is surgical resection followed by focal radiotherapy however; the use of adjuvant chemotherapy at the time of surgery and radiotherapy is widely used (Brandes, 2003).

1.7.1 Surgery

Surgical intervention is the most common form of treatment for glioma and there are several indications for the use of surgery which include reduction of tumour burden, alleviation of mass effect, control of seizures, reversal of neurological deficit, confirmation of histological diagnosis, diversion of cerebrospinal fluid (CSF) by shunting procedures and the introduction of local chemotherapeutic agents (Newton and Jolesz, 2008). Tumours can either be completely or partially resected or biopsied. Even partial resections are beneficial to the patient (Castro *et al*., 2003). When surgical resection is indicated the aim is to remove as much as possible. However; GBM are difficult to resect because of lack of a defined tumour edge, as the tumour often extends into normal brain tissue or may be localized near the critical brain areas. In this respect, radiotherapy is the choice of supplementary therapy to target residual tumour (Brandes, 2003). Recent advances in neurosurgical techniques offer new approaches to tumour removal such as frame-based and frameless stereotactic biopsy, pre-operative functional magnetic resonance imaging (MRI) and intra-operative cortical mapping, neuronavigation, tumour resection in 'awake' patients and the use of intra-operative MRI (Matz *et al*., 1999 and Nimsky *et al*., 2001).

1.7.2 Radiotherapy (RT)

Following surgical resection RT can be used to kill residual tumour cells and several clinical trials have shown this to increase survival in patients with high-grade gliomas (Little and Friedman, 2004). Nieder and collegues (2000) indicated that the survival of patients with various RT techniques is broadly similar, however, considerable toxicity is associated with radiosurgery and brachytherapy therefore, to minimise brain damage caused by high dosage, hyper fractionated external beam RT can be used. This technique delivers more frequent fractions of a smaller dose over a smaller region of the brain. Stereotactic radiosurgery has been developed, allowing delivery of more precise, higher doses RT to a small section of the brain. Brachytherapy can be used if the tumour is well-defined, surgically accessible and <5cm in diameter. This method uses radioactive pellets implanted within the tumour to kill cancer cells and minimise the exposure of normal brain tissue (Nieder *et al*., 2000).

1.7.3 Chemotherapy

Post-operative chemotherapy has been correlated with an increase in survival of patients with high grade glioma (Nieder, 2009). Chemotherapy of brain tumours is not curative and the goals of treatment are mainly to control tumour growth and maintain good quality of life for patient for as long as possible. Cytotoxic drugs used in chemotherapy are developed to kill neoplastic cells or leave them radiosensitive while preserving normal cells. The intact B-BB prevents access to the tumour whereas a disrupted B-BB still provides limited protection for the tumour from chemotherapy therefore various strategies

are available such as intra-arterial, intrathecal and intratumoural as well as disruption of B-BB. The most common chemotherapy drugs are the nitrosoureas. Other agents also used include platinum-based drugs, procarbazine, viscristine- a vinka alkaloid which attacks the nuclear spindle and naturally occurring compounds (Castro *et al*., 2003). Temozolamide (TMZ), an alkylating agent is currently the agent of choice for the treatment for glioblastoma (Stupp *et al*., 2001) and was introduced for general use following an exhaustible major evaluation and re-evaluation by the National Institute for National Excellence (NICE).

The main disadvantage with chemotherapy is that not all tumours are responsive to the drugs used and there may be serious adverse effects. Stewart (2002) assessed the effects of systemic chemotherapy and/or RT on survival and recurrence in adults with high-grade glioma reported a small but clear improvement in survival. One trial has further reported that median survival of patients receiving carmustine polymers (Gliadel wafers) was 31 weeks compared with 23 weeks for patients receiving placebo polymers (Brem *et al*., 1995).

1.7.4 Prognostic Indication and therapeutic response

Another group of therapies include the alkylating agents such as the Procarbazine-Lomustine (CCNU)-Vincristine (PCV) regimen (Oncovin®). The more recently discovered Temozolomide (Temodal®) is also an alkylating agent, its mode of action occurs through its ability to methylate DNA at the N-7 and O-6 positions on guanine residues which subsequently blocks the cell cycle at the G_2-M boundary and triggers

apoptosis (Friedman 2000). However, some degree of resistance to the action of temozolomide on gliomas has been reported and it is thought that the tumour cells expressing the enzyme MGMT exhibit a poor response to temozolomide treatment and such CpG methylation of the *MGMT* promoter (dictating MGMT expression) is a predictive factor of treatment response. Additionally, LOH at 1p 19q in oligodendrogliomas appears to correlate to chemosensitivity and an improved prognosis. Other cell cycle disrupting agents include carboplatin and irinotecan (Simpson and Galanis, 2006).

Agents that act on the mitochondria to induce tumour cell death are few and far between, but the tricyclic Clomipramine (Anafranil®)-originally licensed to treat depression-is one such agent. Its ability to cross the B-BB and target the mitochondria of neoplastic cells but not healthy tissue and without inducing DNA damage indicates its potential as a therapeutic agent in the treatment of glioma but as yet no clinical trials have been carried out and the drug is not generally available to patients.

1.8 Future therapeutic strategies

Standard methods of cancer therapy offer relatively no specificity to malignant lesions and frequently cause serious adverse effects. The revolution in molecular medicine has allowed the development of novel therapeutic modalities, in which cancer-specific changes can be utilized for targeted therapies. The alternative therapies should aim to combat local invasion of tumour cells and develop cytotoxic drugs that can cross the blood brain barrier and be effective against both dividing and migrating cells. Potential approaches include gene therapy, specific molecular targeting, clinical immunotherapy, anti-invasion, anti-angiogenesis, pro-apoptotic strategies and mitochondrial targeting. Molecular targeting therapies hold promise of providing new cancer treatments that are more effective and less toxic than traditional cytotoxic agents.

1.9 CD44

CD44, originally known as the lymphocyte homing receptor, is a multistructural and multifunctional cell adhesion glycoprotein (Naot *et al*., 1997). It has been previously allocated the names Hermes-1, lymphocyte homing receptor, Pgp-1 and extracellular matrix receptor III (Picker *et al*., 1989; Jalkanen *et al*., 1986; Omary *et al*., 1988 and Gallatin *et al*., 1989). The human CD44 gene is located at the chromosomal locus 11p13 and exists as two isoforms. The most abundant standard isoform of human CD44 protein (CD44s or CD44H) contains 363 amino acids and has a molecular weight of ~ 80kDa and the largest possible protein, containing peptides from all variant exons (CD44v or CD44E) is 150kDa (Aruffo *et al*., 1990; Miyake *et al*., 1990; Stamenkovic *et al*., 1991 and

Akiyama, 2001). The standard isoform (CD44s) consists of exons 1-5 and 16-20. The 10 variable exons 6-15 (v1-10) (Hofmann *et al*., 1991; Tolg *et al*., 1993; Screaton *et al*., 1992) are designated CD44v.

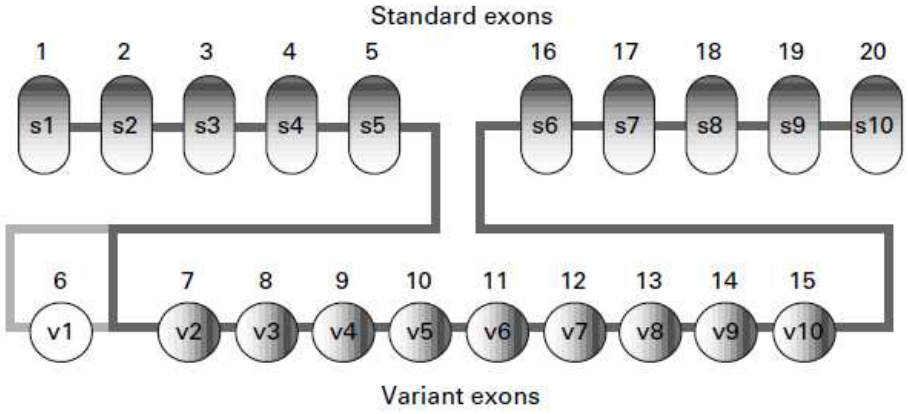

Figure 5: Schematic diagram of the structure of the CD44 gene. The standard exons (s1-10) encode the ubiquitously expressed standard protein isoform, CD44s. combinations of the variant exons (v1-10) can be alternatively spliced between s5 and s6 to encode variant protein isoforms, CD44v. exon 6 (v1) of the human gene contains a stop codon and is not normally included in human mRNA (Goodison *et al*., 1999).

The protein consists of three regions, a 72 amino acid C-terminal cytoplasmic domain, a 21 amino acid transmembrane domain and a 270 amino acid extracellular domain. The cytoplasmic region is encoded by part of exon 18 and by exons 19 and 20 (Goldstein *et al*., 1990).

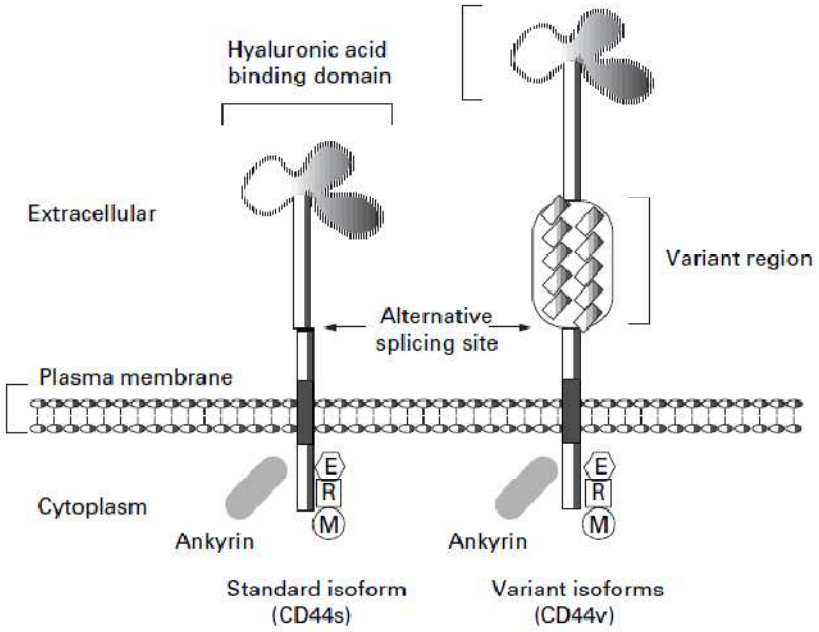

Figure 6: CD44 protein structure, the standard isoform binds its principal ligand, hyaluronic acid at the N-terminal, distal extracellular matrix. The molecule interacts with the cytoskeleton through the binding of ankyrin and the ERM family (ezrin, radixin moesin) to the cytoplasmic domain (Goodison *et al*., 1999)

1.9.1 Expression of CD44

Most mammalian cells predominantly express the CD44s isoform but some epithelial cells also express CD44v/CD44E (Iida and Bourguignon, 1995). The expression of CD44 isoforms containing combinations of the other variant exons (CD44v) is relatively unknown in normal tissues but it is indicative of invasive and metastatic propensity of cancer cells (Bellail *et al*., 2004). However, CD44v has been found in haemopoietic cells (Stauder *et al*., 1995), particularly in peripheral blood mononuclear cells (Salles *et al*., 1993) and in reactive lymph node cells (Arch *et al*., 1992). The expression of CD44v6 has been seen in the ducts of breast (Terpe *et al*., 1994) and pancreas (Gansauge *et al*., 1995;

Hong *et al*., 1995) and CD44v4 is expressed in normal urothelium (Southgate *et al*., 1995). CD44 is expressed in normal astrocytes (Okamoto *et al*., 2002) although the expression is considerably less in comparison with neoplastic astrocytes (Pilkington *et al*., 1993).

Certain cell types, however, do not express any CD44, including hepatocytes, pancreatic acinar cells and cells of the tubules of the kidney and pancreas (Mackay *et al*., 1994).

1.9.2 Function of CD44

CD44 is centrally involved in a wide spectrum of activities notably lymphocyte homing and activation, cell-matrix interactions, cell migration, tumour invasion and metastasis (Okamoto *et al*., 2002) and specifically as a receptor for hyaluronic acid (HA) (Gunthert, 1993). Indeed, the multiple functions reported for the CD44 family of proteins have largely centered around the binding of HA (Culty *et al*., 1992). The various functions reported for CD44 are, in part, also possible by the alternative splicing of the pre-mRNA and the fine tuning of ligand binding (Tolg *et al*., 1993).

1.9.2.1 Role in cell adhesion

The main role of CD44s protein is in the maintenance of three dimensional organ/tissue structure. Upregulation of CD44 and HA production facilitates development of a structural scaffold during epithelial growth and repair (Alho *et al*., 1989; Jain *et al*., 1996). Moreover, a high amount of HA has been found in angiogenesis (Trochon *et al*., 1996), wound healing (Jain *et al*., 1996) and embryonic cell migration (Sherman *et al*., 1996;

Wainwright *et al*., 1996). HA serves as a ligand support for CD44 mediated cell movement and mediates the aggregation of cells by multivalent HA binding by CD44 on adjacent cells or by CD44/CD44 binding via attached glycosylation moieties (Cooper and Dougherty, 1995).

1.9.2.2 Role in neoplasia

The expression of multiple CD44 isoforms and the resulting HA binding profile can influence tumour growth and development. Initial studies showed that tumour tissues contained a number of unusual CD44 transcripts when compared to those in normal tissues (Stamenkovic *et al*., 1989; Stamenkovic *et al*., 1991). Furthermore, it has been demonstrated that tumour cell lines with high level of CD44 proteins were able to form more aggressive tumours in animal experiments (Birch *et al*., 1991; Sy *et al*., 1991). Gunthert (1991) demonstrated in an athymic mouse model that by transfecting plasmids expressing CD44s or CD44v isoforms into non-metastatic, rat pancreatic carcinoma cells, the CD44s gene had no effect in upregulation of metastasis while CD44v expression conveyed metastatic competence to these cells. The ability of the CD44v expressing cells to metastasize was not dependant on HA binding; this was confirmed as a CD44 exon v6 specific antibody that blocked metastasis formation in this system (Seiter *et al*., 1993) did not interfere with HA binding (Sleeman *et al*., 1996). There is also evidence for a correlation between raised CD44 expression and metastatic capability in both cultured human melanoma (Birch *et al*., 1991) and lymphoma cell lines (Sy *et al*., 1991). These

observations therefore, suggest that cell surface CD44 function promotes tumour cell survival in invaded tissues.

1.9.3 CD44 in brain tumours

Data from extensive studies have shown that CD44 is expressed in both neoplastic and reactive astrocytes but over-expressed in neoplastic cells where it aids glioma cell adhesion and invasion (Okamoto *et al*., 2002). In glioblastomas, several species of CD44 mRNA are expressed and encode standard CD44 (Kuppner *et al*., 1992; Pilkington *et al*., 1993). Merzak and colleagues (1994) showed that CD44 is directly involved in human glioma cell invasion, through interaction with extracellular matrix (ECM) components. However, to date, CD44 splice variants occur in brain metastases but not primary brain tumours thus suggesting a specific role of CD44v in metastasis (Li *et al*., 1993). On the other hand, since CD44s has been shown to mediate attachment to a variety of ECM components, including hyaluronate (Pilkington, 1994; Asher *et al*., 1992), CD44-hyaluronate binding would facilitate the migration of cells through the brain ECM. The notion that CD44 being essential for invasion is supported by both *in vitro* and *in vivo* investigations including antisense inhibition of CD44 *in vitro* and the observation that intracranial injection of glioma cells with low CD44 expression levels into nude mice provided localized well-circumscribed neoplasms (Okada *et al*., 1996). Furthermore, monoclonal antibodies directed against CD44 decreased intracerebral invasion of glioma cells both *in vivo* and through *in vitro* matrigel matrices (Gunia *et al*., 1999). Moreover, a proteolytic cleavage of the extracellular portion of CD44 has been shown to occur in gliomas but not in normal

brain (Okamoto *et al*., 1999). In several tumour cell lines, including glioma, this cleavage led to the release of a soluble fragment in the medium and also to a membrane-bound cleavage product (Okamoto *et al*., 1999). *In vitro*, it has been shown that the soluble and the membrane-bound fragments of CD44 promote tumour cell migration (Kajita *et al*., 2001; Okamoto *et al*., 1999).

1.9.4 CD44 and interaction with Hyaluronic acid (HA)

Depending upon tissue type, a range of extracellular adhesive proteins and their receptors on the cell surface are important factors for cell attachment (Bignami *et al*., 1993). Hyaluronic acid and its receptor (CD44) are key players for this role in the brain. HA is one of the constituents of extracellular matrix and is a 85 kDa glycosaminoglycan (Misra *et al*., 2009) present in almost tissues of vertebrates and regulates cellular events such as cell proliferation and locomotion that are required for a variety of biological processes, including tumourigenesis (Cao *et al*., 2006). Tumours often contain high levels of HA which correlates with invasion and increased malignancy in some neoplasms (Merzak *et al*., 1997; Stamenkovic, 1991). HA is particularly over-expressed to approximately four-fold in primary brain tumours (Delpech *et al*., 1993). HA has been shown to facilitate primary brain tumour invasion *in vivo* and migration *in vitro* through its two cellular receptors, CD44 and RHAMM (Receptor for Hyaluronic Acid-Mediated Motility). Antibodies directed against these receptors have been shown to inhibit invasion and migration (Akiyama *et al*., 2001).

The exact mechanism by which CD44 and HA interact to mediate migration and invasion are still under investigation however aggregates of CD44 expression at the interface of normal brain and glioma spheroids appear to link cell membrane surfaces to HA (Merzak & Pilkington, 1997). As part of its diverse cell interactions, HA plays a role in cell detachment from supporting matrices such as ECM. This enables cells to detach, migrate and divide more easily. Studies in animal models demonstrate the injection of reagents that disturb CD44-ligand interaction, which subsequently inhibit local tumour invasion and metastatic spread (Stern *et al*., 2001). Moreover, HA takes on water of hydration, swells and pushes aside the brain tissue to allow CD44/HA mediated tumour cell invasion (Stern *et al*., 2001). Then, subsequently the tumour cells produce and secrete hyaluronidase which breaks down HA. The breakdown products are angiogenic, which induce blood vessels to recruit to the tumour.

1.10 CD155

Poliovirus is a small iscosahedral RNA virus which belongs to the picornavirus family. It was first recognised to mediate binding, poliovirus to host cells, which causes symptoms such as flaccid paralysis characteristic in poliomyelitis (Sloan *et al*., 2004; Sloan *et al*., 2005). The restricted tropism of poliovirus is poorly understood. In addition to the restricted cell and tissue tropism, poliovirus only infects primates and primate cell cultures. Other mammalian species remain unaffected (Ren *et al*., 1990).

The isolation of poliovirus in 1908 and subsequent discovery of the human poliovirus receptor (PVR), as the cellular docking molecule for poliovirus, was followed by the

development of a transgenic mouse expressing the human poliovirus receptor as an animal model for poliomyelitis such as mice, when infected with poliovirus, developed a neurological syndrome histopathologically and clinically identical to primate poliomyelitis (Koike *et al*., 1991).

The poliovirus receptor (PVR) has now been classified as CD155 (Mendelsohn *et al*., 1989). CD155 or human poliovirus receptor (PVR) is a highly glycosylated ~70kDa type Ia transmembrane cell surface glycoprotein molecule that is part of an immunoglobulin superfamily of CAMs (Merill *et al*., 2004; Bottino *et al*., 2003). Its extracellular region contains three immunoglobulin-like domains: an outermost V-like domain followed by two C2-like domains (Mendelsohn *et al*., 1989). The CD155 gene belongs to a subgroup of the immunoglobulin superfamily sharing the general extracellular structure V-C2-C2. CD155 is expressed in four isoforms: hPVRα and hPVRδ are membrane-bound variants that differ only in the sequence of the cell-internal C-terminal domain, while hPVRβ and hPVRγ are secreted isoforms lacking the transmembrane domain (Koike *et al*., 1990; Wimmer *et al*., 1993). hPVRα and hPVRδ are type Ia single-pass transmembrane glycoproteins with apparent molecular weight of >80 kDa, whereas the core polypeptides are 42.5 and 40 kDa respectively. Binding of poliovirus occurs at the V-domain of the polypeptide (Bernhardt *et al*., 1994).

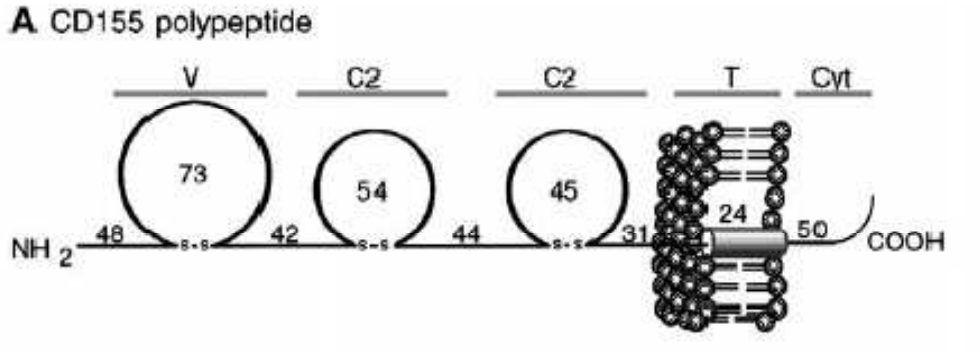

Figure 7: CD155 protein structure. The overall domain arrangement of CD155 is indicated on top. The lengths of individual domains subdivided by the cysteine disulfide bonds characteristic for the IG-like domains are indicated by numbers (Gromeier *et al*., 2000)

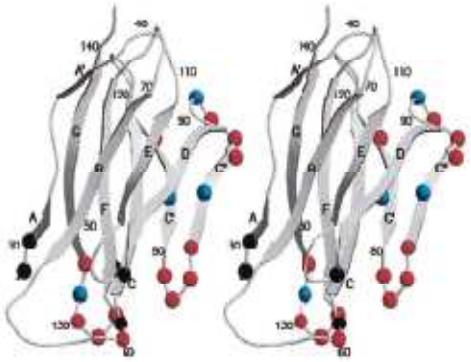

Figure 8: Ribbon diagram of CD155 domain. Residues in the virus-receptor binding interfaces are shown in coloured spheres (He *et al*., 2003).

1.10.1 Expression of CD155

Although previous studies have shown that CD155 is widely distributed throughout human tissues, its level of expression is strictly regulated (Freistadt, 1994; Solecki *et al*., 2000) and it is found only in primates (Aoki *et al*., 1994; Koike *et al*., 1992). CD155 is not highly expressed in adult human brain (Tokuyuki, 2008) but ubiquitous CD155 expression is

confirmed in sites such as the human spinal cord, motor neurons, leukocytes and many human tissues such as kidney, ileum, liver, lung and placenta (Sloan *et al*., 2004; Bernhardt *et al*., 1994). However, CD155 is localised in ECM and at cell-cell junctions but tends to show particularly low levels of expression thus making it difficult to determine exact levels of expression in specified sites (Merrill *et al*., 2004).

1.10.2 Function of CD155

Although the physiological function for CD155 is unknown, the protein was shown to bind specifically to the extracellular matrix vitonectin (Lange *et al*., 2001) and thus classified as a cell adhesion molecule binding protein. Research currently suggests it may play a role as a regulator of cancer invasiveness and glioma migration through its ability to inhibit cell adhesion and enhance cell migration (Sloan *et al*., 2005). Other known molecular functions of CD155 are: protein binding, receptor activity and viral receptor activity. William and Barclay (1988) highlighted that most of the proteins in the Ig superfamily including CD155 are involved in cell-cell interaction during normal or pathological processes such as inflammation, tumourigenesis and cancer metastasis.

1.10.3 CD155 in neoplasia

The first suggestions of a link between CD155 and cancer were centered around the use of poliovirus to infect and destroy human tumour cells. Such neoplastic cells obtained from surgical resections were susceptible to poliovirus while non-malignant cells resisted the

poliovirus. Thus, it is assumed that susceptibility to poliovirus was based on overexpression of CD155 following malignant transformation. The link of CD155 with cancer is further evident from studies of the expression of CD155 during embryonic development. Like many of its fellow members of the immunoglobulin superfamily, CD155 appears to be expressed during embryonic development. Frequently, immunoglobulin superfamily molecules that are expressed in a developmental manner have been associated with malignancy (Walsh *et al*., 1997). More recently CD155 has been identified as a tumour antigen as its expression is up-regulated in neuroectodermal cancers, such as glioblastoma multiforme, medulloblastoma and colorectal carcinoma (Vestweber, 2002 and Weber, 2003).

1.10.4 CD155 in brain tumours

It has been reported that CD155 is over-expressed in malignant gliomas (Gromeier *et al*., 2000) and that increased levels of CD155 are expressed on neoplastic cells from primary brain tumours of several types including GBM (Sloan *et al*., 2004). CD155 expression levels in tumour tissues corresponded to those in primary tissue cultures derived from the tumours. Furthermore, CD155 expression in primary glioma explants cultures was equal to that found in established glioma cell lines used in preclinical evaluations of oncolytic poliovirus recombinants (Merrill *et al*., 2004). Further studies carried out by Sloan and collegues (2004) have revealed that CD155/PVR was highly expressed in both U87 human glioma cells and primary glioblastoma tumour tissue.

1.10.5 CD155 and ECM interactions

Although the exact mechanism by which CD155 controls glioma migration is still unclear, it is postulated that it is recruited to the leading edge of migrating tumour cells and co-localises with integrins and actin, which are involved with the processes of motility and cell-substrate adhesion (Bernhardt *et al*., 1994). More specifically, CD155 binds to vitronectin, which is a major serum protein, abundant in high grade gliomas and an important constituent of the ECM (Lange *et al*, 2001; Ohnishi *et al*., 2007). Vitronectin has further been reported to promote glioma cell survival and invasion (Gladson *et al*., 1995; Uhm *et al*., 1999). CD155 has been demonstrated to bind to vitronectin and additionally co-localise with specific integrins in cancer cells (Sloan *et al*., 2005). It is thought that control of invasion by CD155 maybe substrate-dependent and that by decreasing the stability of focal adhesions at the cell-substrate interface, neoplastic cells become less adherent and more motile (Sloan *et al*., 2005). This proposed interaction establishes an additional link between CAMs and ECM in glioma cells (Lange *et al*., 2001). Further evidence of up-regulation of CD155 expression in glioma cells suggests a potential mechanism which reflects its invasive phenotype which is necessary for cancer progression (Bernhardt *et al*., 1994; Ohnishi *et al*., 2007).

1.11 Association between CD44 and CD155

To date, Freistadt and Eberle (1997) have provided promising evidence that there is a physical association between CD155 and CD44 on the cell membrane of blood monocytes. They demonstrated that anti-CD44 monoclonal antibody (mAb) inhibited the binding of anti-CD155 mAb. Similarly, Shepley and Racaniello (1994) demonstrated that anti-CD44 mAb hindered the binding of poliovirus to CD155 due to its steric position. These studies reflect a close physical apposition between CD155 and CD44. It has been suggested that CD44 may act as a co-receptor for cellular uptake of poliovirus; however the localisation of CD44 in human tissues does not correlate with poliovirus susceptibility (Shepley and Racaniello, 1994). However, such interaction between CD44/CD155 and its implications have yet to be researched with respect to brain tumours. In particular work on the role of CD155 in brain tumour is still in its infancy and its possible role as a therapeutic target for invading tumour cell populations in primary brain tumours remains to be explored. However, if a similar juxtaposition of CD44 and CD155 as has been reported on monocytes could be observed on brain tumour cells, this might further indicate that CD44/CD155 plays an interactive role, possibly in conjunction with certain integrin subunits at the tumour cell surface, resulting in mediation of brain tumour invasion via the underlying cytoskeleton. An intimate knowledge of interactive process underlying invasiveness, including those which include CD44 or CD155 may prove valuable in the development of new therapeutic strategies.

1.12 F-Actin

Actin, one of the major components of the cytoskeleton is a structural, roughly 42 kDa conserved protein in eukaryotic cells (Rao *et al*., 1990). Its main importance is in regulation of cell shape, motility, secretion, intracellular transport and cell division (Wessells *et al*., 1971 and Pollard *et al*., 1986). Actin exists in the cytoplasm as either G-actin monomers or F-actin filaments. G-actin (globular actin) with bound ATP can polymerise to form F-Actin (Filamentous Actin) (Rao *et al*., 1991). Actin levels may reflect cancer-related changes at molecular level through several mechanisms including a point mutation in the actin gene and altered regulation of F-actin assembly (Hunter, 1984; Magargal, 1986; Akiyama *et al*., 1988; Holme *et al*., 1986 and Marchisio *et al*., 1987).

1.13 Signal transduction pathways

1.13.1 Rho GTPases

Cells receive various chemical (cytokines and growth factors) and physical (mechanical stress or adhesion to extracellular matrix) stimuli that influence cell function by affecting intracellular signaling pathways (Bushsbaum, 2007). These stimuli usually involve cell surface receptors or other molecules that function through activation of the Rho family of small GTPases. Rho GTPases are members of the Ras superfamily of small GTPases that play a pivotal role in controlling multiple cellular processes, including integrin engagement (Ridley *et al*., 1992; Hall, 1998; Nobes *et al*., 1995; Del Pozo *et al*., 2002) and assembly and organisation of the actin cytoskeleton (Symons *et al*., 2009).

To date more than 20 members of the Rho GTPases family have been identified (Wennberg and Der, 2005) including Rho (RhoA, RhoB, RhoC), Rac (Rac1, Rac2, Rac3) and Cdc42 (cell division cycle 42) (Bishop & Hall, 2000; Ridley, 2001; Boettner and Van Aelst, 2002; Ridley *et al*., 2003; Burridge & Wennerberg, 2004; Jaffe & Hall, 2005) (Figure 9). RhoA, RhoB and RhoC are Ras homolog gene family members A, B and C respectively. Rac1, Rac2 and Rac3 are Ras-related C3 botulinium toxin substrate 1, 2 and 3 respectively.

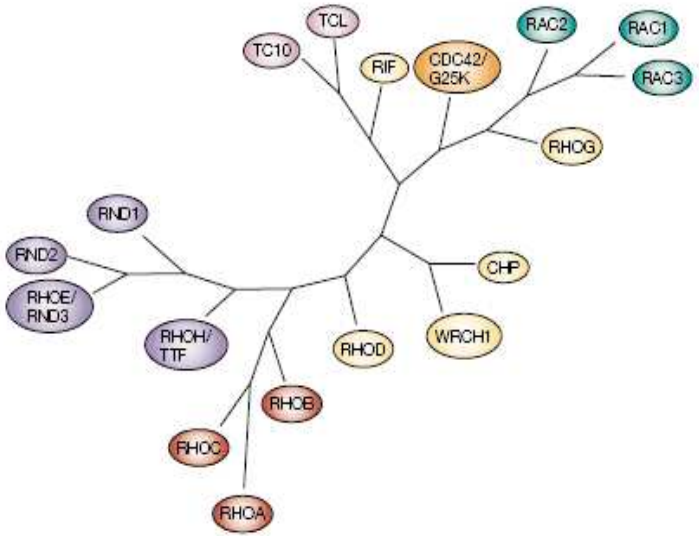

Figure 9: The RHO-protein family. The RHO proteins can be subdivided on the basis of functional, biochemical and sequence data. The subgroups include proteins that are most similar to RhoA, those that are most similar to RAC1 and CDC42, and those that lack GTPase activity. The RND proteins and RHOH have been grouped together because of their predicted lack of GTPase activity (Sahai and Marshall, 2002).

Rho GTPases proteins act as molecular switches that cycle between inactive GDP-bound and an active GTP-bound state (Figure 10). In the GTP-bound active state, Rho GTPases interact with target proteins known as effectors to induce a cellular response until GTP hydrolysis returns them to the GDP-bound inactive state. The interconversion between the GDP-bound to the GTP-bound state is mediated by a large family of guanine-exchange factors (GEFs) that increase GDP/GTP exchange rates and GTPase-activating proteins (GAPs) that elevate the intrinsic GTPase activity of Rho GTPases (Hall *et al*., 2005).

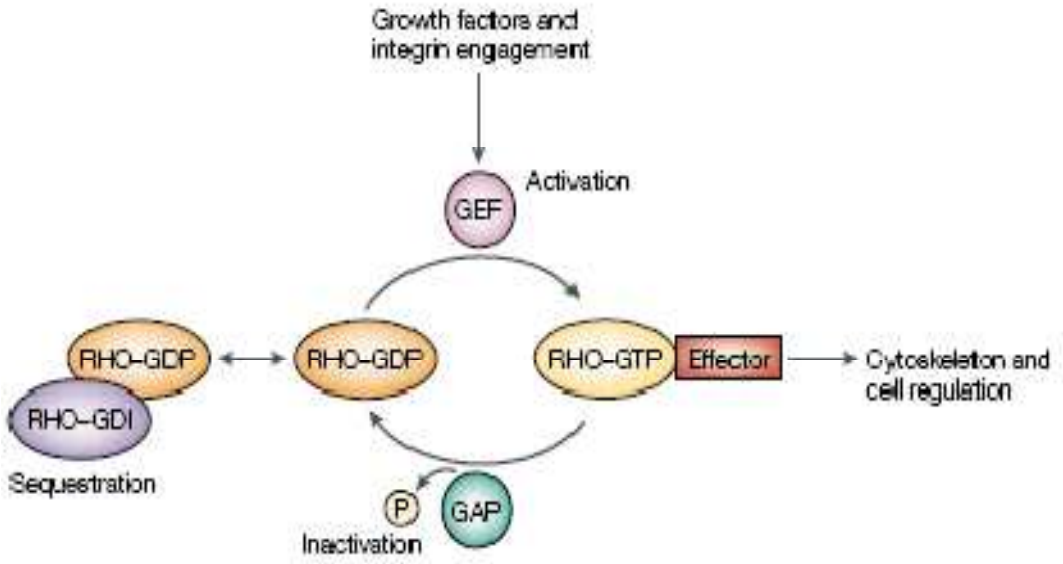

Figure 10: Model of RHO-protein regulation. RHO proteins can bind either to GTP or GDP. When bound to GDP, they can be sequestered in the cytoplasm by RHO-GDP dissociation inhibitors. The exchange of GDP to GTP is promoted by RHO by guanine nucleotide exchange factors and is often associated with translocation of RHO proteins to proteins cell membranes. GTP-bound RHO proteins interact with a range of effector proteins and modulate their ability to regulate cell behaviour. Most RHO proteins have an intrinsic ability to hydrolyse GTP to GDP and inorganic phosphate (P), which can be promoted by RHO-GTPase-activating proteins (Sahai and Marshall, 2002).

1.13.2 Rho GTPases in invasion

Invasion is a complex process that relies on the spatial and temporal organization of actin dynamics, adhesion and protease activity. Regulation of the actin cytoskeleton, formation of membrane projections and assembly of specialized adhesion complexes in glioma invasion may all be mediated through Rho family members (Banyard *et al*., 2000). Indeed, Rho family proteins have distinct roles in regulating the actin cytoskeleton and the formation and regulation of actin-rich protrusive structures that are actin-containing membrane structures that mediate different aspects of cell motility and adhesion (Hotchin and Hall, 1995). Rac1 is known to regulate actin polymerisation at the cell periphery to produce the sheet-like lamellipodia and the ruffles. Cdc42 promotes actin filament assembly to induce the formation of thin finger-like filopodia. Rho is required for the formation of contractile actin-myosin filaments, also known as stress fibres, and regulates the formation and maintenance of focal adhesions (Ridley *et al*., 1992; Hall *et al*., 2005). Normally low levels of Rac1 induce lamellipodia/ruffle formation at the two extremities of the main axis whereas higher levels of Rac1 induce lamellipodia/ruffles around the whole perimeter of the cell (Pankov *et al*., 2005). Rac is also involved in cell spreading and integrin-dependent adhesion to the extracellular-matrix (D'Souza-Schorey *et al*., 1998). Temporal and spatial controlled Rac1 activation is also important in different phases of cell-cell adhesion (Ehrlich *et al*., 2002; Cascone *et al*., 2003).

It is most probable that Rho proteins play a role in the invasive phenotype of tumour cells (Figure 11) knowing that they are involved in the regulation of cell motility in normal cells and their peculiar regulation in tumour cells. While many *in vitro* studies show that Rho proteins are involved in cell motility; precisely how Rho proteins promote

invasion/metastasis remains to be elucidated. RhoC and its effector ROCK have however, clearly been shown to be implicated in *in vivo* models of tumour-cell dissemination (Clark *et al*., 2000; Itoh *et al*., 1999; Murata *et al*., 2001; Somiyo *et al*., 2000).

It is postulated that the mechanism of invasion by the Rho proteins is as follows: Rho proteins are involved in the loss of epithelial polarity and are thought to be determinant in the epithelial-mesenchymal transition that is occasionally observed in aggressive tumours. Normal epithelial sheets are characterised by cell polarity and a well-organised array of specialized cell-cell junctions such as adherens and tight junctions. High levels of RND3/RhoE, which antogonises RhoA function (Guasch *et al*., 1998; Nobes *et al*., 1998) can promote a loss of polarity and multilayering of epithelial cells (Hansen *et al*., 2000). On the other hand, inhibition of Rac1 leads to a loss in polarity resulting in the non-deposition of laminin asymmetrically (O'Brien *et al*., 2001). Data collected by Kim (2000) showed the association of Rac1 with the mammalian orthologues of the *Caenorhabditis elegans* cell-polarity genes *par3* and *par6* might also be involved in controlling epithelial-cell polarity. Additionally, the downregulation of Rac1 activity of RAS-transformed or phorbol-ester-stimulated Madin-Darby canine kidney (MDCK) cells leads to the loss of epithelial-cell junctions and a more mesenchymal and motile phenotype (Zondag *et al*., 2000). In some cells, activation of Rho proteins can contribute to the loss of adherens junctions; in fact, the ability of TGF-β to promote the loss of adherens junctions is dependent on Rho and ROCK function (Bhowmick *et al*., 2001) and in keratinocytes, active Rac1 leads to the dis-assembly of adherens junctions (Braga *et al*., 2000). Furthermore, increased motility and the ability to remodel the ECM are required for tumour cells to become locally invasive. RhoA and Rac1 can regulate the function of ezrin

(a characteristic of astrocytes (Pujuguet *et al*., 2003), moesin (localised to filopodia and membraneous protrusions that are important for cell-cell recognition, signalling and for cell movement) and radixin (links actin to plasma membrane): these related proteins are known to promote cell motility by linking the actin cytoskeleton to the plasma membrane through CD44. RhoA promotes phosphorylation of ezrin by ROCK leading to its increased association with the cytoskeleton (Matsui *et al*., 1998) whereas Rac1 promotes the phosphorylation and inhibition of the ezrin antagonist neurofibromatosis 2 (Shaw *et al*., 2001; Xiao *et al*., 2001). RhoA and Rac1 can modulate the degradation and remodeling of the ECM either by regulating the levels of matrix metalloproteinases (MMPs) that degrade the ECM or by regulating the levels of their antagonists, tissue inhibitors of metalloproteinases (TIMP) (Zhuge *et al*., 2001; Engers *et al*., 2001; Kheradmand *et al*., 1998; Matsumoto *et al*., 2001). The ability to enter either the blood or the lymphatic vasculature is required for tumour cells to metastasize to distant sites. RhoA and ROCK are required in both the endothelial and the migrating cells for them to cross the vascular endothelium (Worthylake *et al*., 2001; Adamson *et al*., 1999). It was demonstrated that overexpression of RhoC leads to increased levels of angiogenic factors in breast epithelial cells (Van Golen *et al*., 2000) which could lead to increased vascularisation of the tumour and increased likelihood of tumour cells to enter the blood stream. High levels of RhoC also promote the ability of melanoma cells to exit the blood and colonise the lungs (Clark *et al*., 2000).

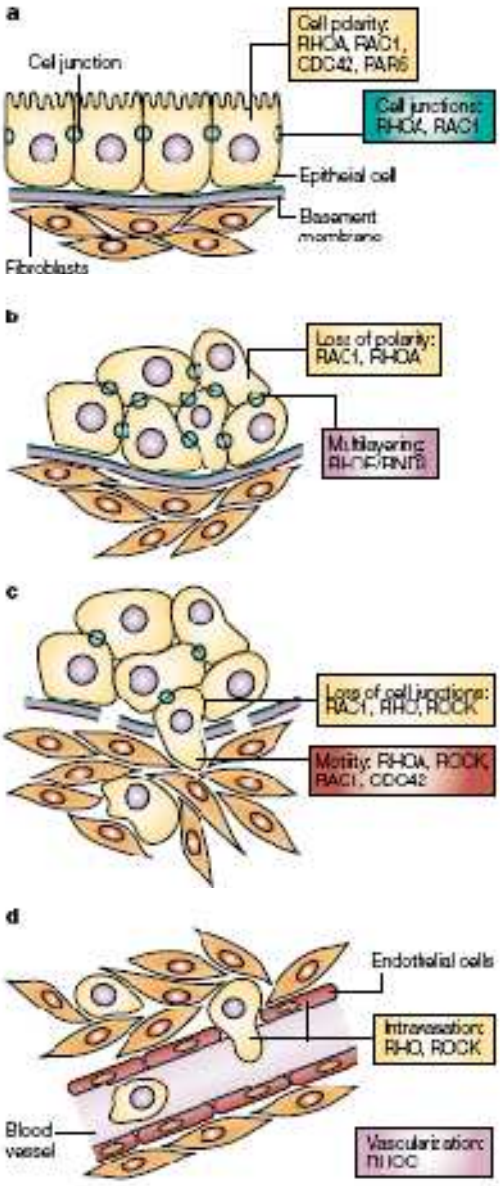

Figure 11: Involvement of RHO proteins at different stages of tumour progression. (a) maintenance of normal epithelial polarity. (b) benign tumours: loss of polarity and multilayering. Inhibition of RAC1 leads to failure to deposit laminin asymmetrically and subsequent loss of polarity. Activation of RHOA also leads to loss polarity but antagonism of RHOA function by RHOE/RND3 overexpression which leads to multilayering of epithelial cells (c) locally invasive tumours: loss tissue boundaries and increased motility-modulation of RAC1 and RHO/ROCK activation can lead to loss of cell-cell junctions. Elevated activity of RHOA, ROCK, RAC1 regulate expression of proteases that facilitate motility by degrading the basement membrane and other extracellular matric compounds (d) metastasis to distant site: intravasation and extravasation. RHO and ROCK are required for tumour cells to cross endothelial cell layers. RHOC promotes expression of angiogenic factors, leading to an increase in vascularisation of the tumour (Sahai and Marshall, 2002).

1.13.3 Rho GTPases in brain tumours

The Rho-family GTPases namely Cdc42, Rac1 and RhoA are major regulators of actin cytoskeletal organization and play a crucial role in many cellular processes, including cell migration (Etienne-Manneville and Hall, 2002; Nobes and Hall, 1999). All three of these GTPases have also been shown to influence invadopodia regulation although in different cell types (Berdeaux *et al*., 2004; Chuang *et al*., 2004; Yamaguchi *et al*., 2005). In glioma cells namely SNB-19 and U87MG, depletion of Rac1 or its effector, synaptojanin 2, using siRNA inhibited invasiveness of cells through slices of rat brain tissue and through matrigel (Chuang *et al*., 2004). Senger and collegues (2002) showed that Rac1 regulated an important survival pathway in most glioma cells and that suppression of Rac1 activity stimulated the death of almost all glioma cells irrespective of p53, MDM2 or EFGR mutation or amplification status. The results thus suggest that mutation in effector region of Rac1 gene may be related with some brain tumours of different metastasic potential (Hwang *et al*., 2004). Rac 1 is known to be a critical regulator of glioma motility and invasion (Salhia, 2006).

It has been reported that there is an increase of RhoA expression in high-grade astrocytomas (Yan *et al*., 2006). RhoA and RhoB expression is, however, inversely correlated with tumour grade in glioma (Forget *et al*., 2002). In addition, inhibition of ROCK has been reported to increase motility of GBM cells with associated membrane ruffling and collapse of actin fibres (Salhia *et al*., 2005). Furthermore, recent data have shown that the suppression of GBM cell motility by olig2 occurs via activation of RhoA (Tabu *et al*., 2007).

Studies by Mira and colleagues (2000) showed that Rac3 was overexpressed in 33% of meningiomas, 17% of pituitary adenomas and 9% astrocytomas and that the higher expression of Rac3 in meningiomas may be related to the involvement of a steroid hormone receptor in meningioma biology. Later, the expression of Rac3 was also found in glioblastoma multiforme, raising the possibility of a functional role of Rac3 in this tumour (Hwang *et al*., 2005). This may further suggest that high expression of Rac3 is related to aggressive behaviour of both meningioma and astrocytoma.

1.14 Plan of investigation

The precise location of CD44 and CD155 will be established in a range of human biopsy-derived GBM cell cultures. In the second part of the project, the effects of siRNA 'knock-down' of CD44 and CD155 both individually and in combination will be evaluated in the context of the degree of invasion of brain tumour cells. The interactions of silenced CD44 and CD155 with subunits of integrins will be examined as well as their effects on RHO GTPases signaling pathway.

1.14.1 Hypotheses

1. That the poliovirus receptor (CD155) influences brain tumour cell invasion.

2. That a co-operative role exists between the hyaluronic acid receptor (CD44) and poliovirus receptors (CD155) in modulation of tumour cell invasion.

1.14.2 Aims

1. To characterise the expression of CD44 and CD155 both qualitatively and quantitatively on range of human biopsy-derived GBM cell cultures and non-neoplastic astrocytes.

2. To show whether the two molecules are located closely on the cell membrane of human biopsy-derived GBM cell cultures.

3. To demonstrate that CD44 and CD155 expressing cells demonstrate an invasive phenotype in human biopsy-derived GBM cell cultures.

4. To show that inhibition of these two molecules results in modification of invasive behaviour in human biopsy-derived GBM cell cultures.

5. To show that inhibition of CD44 and CD155 results in alterations in migration and velocity of cell movement.

6. To demonstrate that inhibition of CD44 and CD155 results in altered proliferative rate of GBM cell cultures under study.

7. To show that knock-down of CD44 and CD155 causes differences in adhesion potential on different extracellular matrices.

8. To show the interactions of CD44 and CD155 with F-actin and different subunits of integrins.

9. To show that inhibition of CD44 and CD155 affects the expression level of RHO GTPase proteins.

1.14.3 Objectives

The aims will be carried out by:

1. Characterisation of level of expression and respective distribution of CD44 and CD155 by single and double staining in the following glial/glioma cell lines: UPAB, UPMC, SNB-19 (gliomas) and CC-2565 (non-neoplastic astrocytes) by flow cytometry and ICC using appropriate antibodies to CD44 and CD155.

2. To examine cells with a Zeiss Aviovert microscope incorporating total internal reflected fluorescence (TIRF) to permit high signal, low noise-fluorescence imaging of the CD44 and CD155 epitopes within tumour cell membranes with great clarity and resolution.

3. To assess the invasive potential of CD44 and CD155 through 8µm porosity Transwell^{TM} Boyden chamber filters and characterise the invasive cells by ICC detection with alkaline phosphatase substrate.

4. To determine whether by blocking CD44 and CD155 with specific monoclonal antibody both in combination or individually, invasion was inhibited using a Transwell^{TM} Boyden chamber system.

5. To establish whether the RNAi knockdown of CD155 in glioma cells alters cell morphology with resultant reduction in migration and to enable tracking

directionality and speed of movement through the live cell (time-lapse) microscopy.

6. To assess the adhesive potential of CD44 and CD155 through a fluorometric adhesion assay on untreated cells versus MAb blocking and siRNA- treated cells.

7. To investigate whether MAb blocking and siRNA- treated cells of CD44 and CD155 have an effect on proliferative rate of cells assessed by BrdU proliferation assay.

8. To evaluate the interactions of integrins and F-actin on CD44 and CD155 silenced cells using confocal microscopy.

9. To investigate the molecular mechanisms and effects of GTPase activation in CD44 and CD155 siRNA ‘knockdown’ cells by Western blotting.

CHAPTER TWO

MATERIALS AND METHODS

2.1 Human authentication PCR

Hughes and colleagues (2007) pointed out that cellular cross contamination with other cell lines and even species contribute to misleading results. Thus, to confirm that the short term and long term cell cultures were of human origin and had not been contaminated with mouse or rat cells, the TEST-IT^{TM} Kit from Microzone Ltd (Haywards Heath, UK) was used. The whole experiment and testing of the cell lines was performed by Dr Samantha Higgins (PhD).

2.1.1 Mitochondrial DNA extraction

Mitochondrial DNA was first extracted from the cells using *micro*LYSIS®-PLUS (MLP) (Microzone, Ltd, UK). Cells were harvested and $1x10^4$ cells were then mixed with 20 µl MLP and the total volume made up to 30 µl using MLP. The negative control was 10 µl water added to 20 µl MLP and the positive human control DNA was supplied by Microzone Ltd. Samples were then placed in the thermal cycler (Px2 Thermal cycler, Thermo Electron Corporation).

The cycling profile was as follows (1x cycle):

Step 1: 65^0C for 15 minutes

Step 2: 96^0C for 2 minutes

Step 3: 65^0C for 4 minutes

Step 4: 96^0C for 1 minute

Step 5: 65^0C for 1 minute

Step 6: 96^0C for 30 seconds

Step 7: 20^0C hold

After cycling, the extracted DNA was used for further PCRs or stored at -20^0C for future use. Throughout this protocol all apparatus and molecular grade water (Sigma Aldrich, UK) used were sterile and DNAse/RNAse-free.

2.1.2 Preparation of controls for PCR

Human DNA controls were supplied by Microzone Ltd, mouse and rat DNA controls were produced in-house from mouse and rat tails under Home Office Animals (Scientific) Act 1986 (UK) (Higgins *et al*., 2010). The extraction of genomic DNA from mouse and rat tails was achieved by utilizing the 'Quick Extraction of Genomic DNA from Mouse Tail Kit' (BioPioneer Inc, USA). Small sections approximately 0.2cm were cut from both mouse and rat tails and placed in 100µl of solution A and incubated at 96^0C for 30-60 minutes. The sample was chilled to room temperature and vortexed to mix. 100µl of solution B was added to the samples and vortexed again to mix. 1-2µl of this mixture was then used to run PCR amplification directly or stored at -20^0C.

2.1.3 TEST-IT™ Kit

The TEST-IT™ kit (Microzone Ltd, UK) consisted of MegaMix~Gold (MMG) and PrimerMix 3* (PM3*) and a 100 base pair (bp) DNA ladder for one test; 12.5µl MMG + 10.5µl PM3* was required to make the working mix. For multiple tests, volumes

calculated were multiplied by sample number plus one. 2µl of DNA to be tested (0-10ng) (or 2µl water for the blank) was added to 23µl working mix and placed in the thermal cycler.

The amplification was as follows:

Initial denaturation step: 95^0C for 5 minutes then cycled 30 times:

Step 1: 95^0C for 30 seconds

Step 2: 63^0C for 30 seconds

Step 3: 72^0C for 45 seconds

Step 4: 20^0C hold

2.1.4 Gel Electrophoresis of PCR Products

Reagents: Stock solution **50X TAE buffer** (Tris-acetate +EDTA)

242g TRIS (hydroxymethyl)aminomethane (Sigma Aldrich, UK)

57.1ml Glacial Acetic (Sigma Aldrich, UK)

100mls EDTA 0.5M (pH 8) (Sigma Aldrich, UK)

100 mls EDTA 0.5M (pH 8)

18.61g EDTA (Sigma Aldrich, UK)

80mls dH_2O (in-house)

Adjust with NaOH (Sigma Aldrich, UK) to pH 8 and make up to 100 mls

After cycling, 10µl of PCR product + 4µl DNA loading buffer (Bioline, UK) was loaded onto a 1.7% agarose gel and electrophoresed alongside 10µl of the 100bp ladder. The bio-Rad 'sub cell' was utilized for all agarose gel electrophoresis work.

1.7% agarose gel (Bioline, UK) =1.9125g agarose in 2.25 mls 50x TAE Buffer + 110.25 mls molecular grade distilled water. This solution was placed in a microwave oven for approximately 2 minutes until boiling and cleared. Once the solution had cooled enough to handle, 3µls (10mg/ml) ethidium bromide (Promega, UK) was added before the gel polymerized to enable DNA visualization under ultraviolet light. After casting, the gel was allowed to solidify for approximately one hour. The gel was placed into the tank and 600 mls of 1x TAE buffer was added, the comb was then removed from the gel. Samples were loaded onto the gel and run at 90 volts for 1 hour. The gel was examined under UV light and visualized on the 'Chemi Genius' bio imaging system and imaged using the software Genesnap (Syngene, UK). An image was captured after adjusting for sharpness and light intensity and the size of the separated fragments was estimated by comparing to the species controls and the 100bp DNA ladder.

The expected fragment sizes for the human authentification PCR were as follows:

- DNA from human: 200, 300 and 500bp
- Mouse DNA: 150, 350 and 500bp
- Rat DNA: 250, 450 and 500bp

2.2 Cell culture and cell lines

All cell culture work was carried out aseptically in a sterile laminar flow cabinet (NUAIRE^{TM} Biological safety cabinets, Class II). All glasswares used for tissue culture was previously autoclaved to ensure sterility. All materials to be used in the cabinet were sprayed with 70% ethanol (prepared in-house) to maintain a sterile environment. Cell lines used were cultured in complete medium: Dulbecco's Modified Eagle Medium (DMEM-without pyruvate, with Glucose, Glutamax and Phenol Red) (Gibco, UK), supplemented with 10% heat-inactivated foetal calf serum (FCS) (Sigma Aldrich, UK). Subsequently, cells were passaged to fresh culture flasks: T25 and T75 (Greiner Bio One, UK) every 3-5 days, uplifting cells with TrypLE^{TM} Express (Invitrogen, UK) after washing with Hank's Balanced Salt Solution (HBSS) (Invitrogen, UK). Cell cultures were maintained in a humidified incubator (NUAIRE^{TM} DH AUTOFLOW CO_2 Air-Jacketed) supplied with 5% CO_2 and 95% air at 37^0C. The passage number of the cells was increased by one on subculturing.

Table 2 Primary cell cultures and cell Lines used

Cell Lines	Histological Grading & characteristics	Sex of Patient	Age of patient at time of surgery
CC-2565	Non- Neoplastic Human Foetal cerebral Astrocytes	Male	18 weeks
UPAB	Low passage, heterogenous Grade IV GBM	Male	72 years
UPMC	Low passage, heterogenous Grade IV GBM	Female	68 years
SNB-19 /U251MG	High passage, established Grade IV GBM	Male	75 years

Table 2 shows low passage cell cultures, denoted with 'UP' were established 'in house' from biopsies received from surgical resections. SNB-19 was purchased from the DSMZ German Brain Tumour Bank, Germany and CC-2565 were from Lonza, UK.

2.2.1 Establishment of Primary Cultures

Human tumour biopsies were obtained from excised gliomas or from biopsies of tumours of patients from King's College Hospital (London, UK), with ethical approval obtained; LREC 00-173 and 02-056. On receipt, biopsies were transferred to a sterile petri dish and rinsed with HBSS. Blood clots, blood vessels and necrotic tissues were removed with sterile scalpels; the tissue was then dissected into small fragments until a uniform suspension was obtained. The suspension was then transferred into T25 tissue culture flasks containing DMEM + 20% FCS + 1% penicillin/streptomycin (Invitrogen, UK), left to adhere for 3-4 days. On day 4, the media was removed and washed with HBSS.

Subsequent cells were visualised using an Olympus 1X71 inverted Phase Contrast Microscope. All primary cultures used were established in this way at the University of Portsmouth except CC-2565 (purchased from Lonza, UK) and SNB-19 (DSMZ German Brain Tumour Bank, Germany).

2.2.2 Cryopreservation of cell cultures

Recovery^{TM} cell culture freezing medium (Invitrogen, UK) was supplied complete with dehydrating agent DMSO. This agent is a cryoprotective as it reduces the water content of the cells thus reducing ice crystal formation and hence preventing damage to cell membranes. Cells were harvested as previously described, centrifuged and resuspended in 1 ml of freezing medium which was then transferred to a cryotube. Cell freezing began within 5 minutes of this point; the cryotubes were placed in a 'Mr Freezy', a controlled freezing container which allowed the cells to cool at a rate of 1^0C/minute; in a -80^0C freezer overnight. Afterwards the cells were immersed in liquid nitrogen at -196^0C and stored for an indefinite period.

2.2.3 Resurrection of cells from liquid nitrogen tank

Required cells were taken from liquid nitrogen tank, thawed rapidly at 37^0C and cultured to a T75 tissue culture flask where 9 mls of complete medium was added in a drop-wise manner to avoid the cells bursting due to changes in osmolarity. Media was changed after

24 hours incubation to remove dimethyl sulfoxide (DMSO), returned to the incubator for storage and maintained in a normal way until 80-100% confluency was reached.

2.2.4 Cell counting and seeding densities determination

It is important to determine the number of cells within a flask before beginning any experiment, as per required for certain procedures. An automated ViCell^{XR} Cell Viability Analyzer (Beckman Coulter, UK) utilising the trypan blue exclusion assay was used to determine cell number and cell viability. The protein binding dye, Trypan Blue is taken up passively and retained by dead cells. In this way, dead cells can be differentiated from viable ones and the machine can distinguish between these to give an accurate quantification of cell number and viability. To perform a routine count, cells were harvested, centrifuged and resuspended in 1 ml of complete media from which 100 µl of cell suspension was removed and placed in a sample cuvette with 500 µl of complete media. This was then transferred to the ViCell analyser and the cell count carried out. To determine the volume of cell suspension required for a pre-determined cell number (seeding densities) to start an experiment, the following equation was used:

$$\frac{1000 \times (\text{Number of cells required})}{\text{Total number of viable cells counted}} = \text{required volume (µl) of the cell suspension.}$$

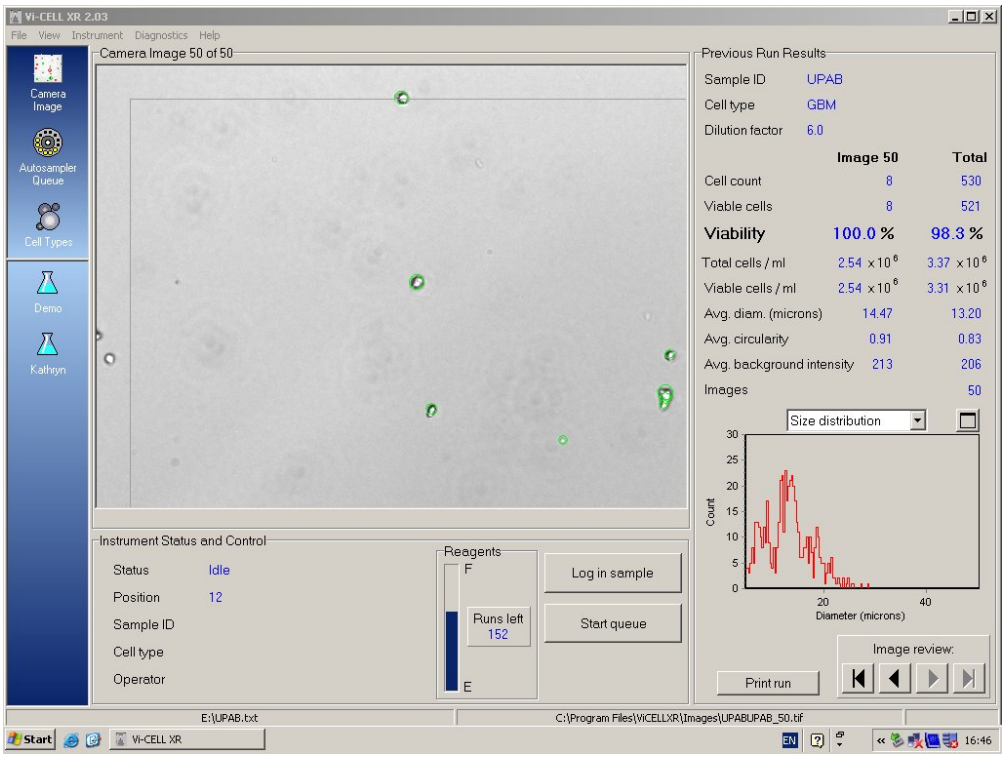

Figure 12: Vi-CELL^{TM} XR data collected for UPAB cells. The total viable cell count was 3.31 x 10^6 cells/ml and the percentage viability was 98.3%.

2.2.5 Growth curves

Growth curves were used to monitor cell growth and consistency of cells. This technique helped to know optimal time to passage cells, determining correct seeding densities and plating efficiency. From a growth curve, the lag time, population doubling time (log or exponential phase) and the saturation density (stationary phase or plateau) can be determined.

Cells were harvested, counted using the ViCell ^{XR} Cell Viability Analyser and initially plated at three different concentrations: 1x10^3 cells; 1x10^4 cells; 1x10^5 cells in triplicate in

T25 flasks for each concentration to determine the optimal seeding density of each cell line used in the scope of this thesis and this procedure was considered as Day 1. The flasks were then returned in the incubator. Sampling was repeated at 24 hour intervals until a plateau was reached (no increase in cell concentration noted in the flasks). The resulting cell densities were plotted against time and the population doubling time (PDT) calculated.

2.3 Flow cytometry

Cells were harvested, centrifuged, resuspended in 1ml PBS (Sigma Aldrich, UK) + 5% FCS (Sigma Aldrich, UK) and split into four eppendorf tubes. Four eppendorf tubes were sufficient to allow one antibody stain in triplicate and a negative control; all tests were repeated at least three times. The eppendorf tubes were centrifuged at 1000 rpm/100g using an Eppendorf 5415R microfuge for 5 minutes, the supernatant discarded and the samples incubated with 100µl cytofix/cytoperm solution (BD Biosciences, UK) for 20 minutes at 4^0C (except for extracellular/cell surface antigens which do not require permeabilisation and so cytofix/cytoperm was **not** used). This allows the permeabilisation of membranes in order to allow interaction of the antibody with its intended target. Samples were then subjected to washing with 500µl PBS prior to incubation with 100µl pre-diluted primary antibody for 40 minutes at 4^0C. This step was omitted for the negative control samples. Samples were washed with 500µl buffer (PBS + 5% FCS), centrifuged and the supernatant discarded. Samples were then resuspended in 100µl secondary Alexa Fluor 488 (Invitrogen, UK) conjugated antibody for 20 minutes in the dark at 4^0C. Samples were then washed, centrifuged and the supernatant discarded. Cell pellets were resuspended in 300µl

(test samples) and 500 µl (control samples), transferred to FACS tubes (BD Biosciences, UK) and analysed. Before analysis, 5µl propidium iodide (PI) (Sigma Aldrich, UK) was added to samples probing cell surface antigens, in order to stain the nucleus, therefore gating out the dead population of cells (except for intracellular antigens which do not require PI). To statistically validate the results, each sample was assayed in triplicate (1 control + 3 positives) in at least three independent experiments.

Analysis was performed on a four colour multi parameter BD Biosciences FACS Calibur equipped with a 488nm argon gas laser and a 635nm red diode laser. Emission fluorescence was collected via a system of optical mirrors and filters and the specified wavelengths of the collected light routed to designated optical detectors. For Alexa Fluor 488/FITC, this was measured using a 530/30nm filter and emission fluorescence for PI was measured using a 670nm LP filter. Acquisition/analysis was performed using CellQuest Pro software.

Table 3 Primary and Secondary Antibodies used for Flow cytometry

Primary Antibody	Dilution	Company	Secondary Antibody	Dilution	Company
CD44	1:25	Chemicon	Goat anti-mouse Alexa Fluor 488 IgG	1:500	Invitrogen
CD155	1:20	R&D Systems	Goat anti-mouse Alexa Fluor 488 IgG	1:500	Invitrogen
GFAP	1:20	Dako	Goat anti-rabbit Alexa Fluor 488 IgG	1:500	Invitrogen
β_1 integrin	1:70	Abcam	Goat anti-rabbit Alexa Fluor 488 IgG	1:500	Invitrogen
F-Actin-conjugated 488	1:40	Invitrogen	Goat anti-mouse Alexa Fluor 488 IgG	*Pre-diluted by the supplier*	

Table 3 lists the details of primary and secondary antibodies with their corresponding species and dilution used for flow cytometry.

2.3.1 Statistical analysis

Statitistical analysis was performed on the data using one-way ANOVA followed by Tukey's multiple comparison post test with a probability of less than 0.05 being regarded as significant. The software package GraphPad Prism 3.02 was used to calculate the statistical tests where all data are expressed as mean values.

2.4 Immunocytochemistry

Cells were harvested from confluent tissue culture flasks and seeded onto sterile 13mm glass coverslips (VWR, UK) within a six well plate at an approximate density of $1x10^5$ and allowed to reach 70-80% confluency before immunostaining. Cells were fixed with 4% paraformaldehyde (PFA) (Sigma Aldrich, UK), pH 7.4 for 5 minutes with three subsequent washes in PBS before proceeding to immunocytochemistry. Prior to primary antibody incubation, cells were blocked with 10% normal serum (species dependent on secondary antibody used) in PBS for 1 hour with 0.2% Triton X-100 (Sigma Aldrich, UK) for 10 minutes at room temperature (except extracellular antigens which do not require permeabilisation thus **no** Triton X-100 was used). All antibodies were diluted in blocking solution and primary antibodies were incubated for one hour at room temperature. Secondary conjugates were incubated at 1:500 dilution at room temperature in the dark for 30 minutes. Nuclei were counterstained with Hoechst Blue (Sigma Aldrich, UK) diluted 1:100 for approximately 20 seconds before coverslips were mounted with Vectashield® (Vectorlabs, UK). Washes were carried out in PBS (5 minutes x 3) before and after each antibody incubations and where double

immunolabelling was carried out, antibodies (raised in different hosts) were cocktailed for both incubation steps. For the control, no primary antibody was added followed by secondary antibody and the specificity of the antibodies were tested as follows:

CD44: Same antibody purchased from different companies and tested through ICC and Flow cytometry.

CD155: C6 glioma cells were stained for CD155 (used as control and specificity since CD155 is only expressed in primates)

Table 4 Primary and secondary antibodies used with their corresponding blocking and buffers

Primary Antibody	Dilution	Species	Secondary Antibody	Dilution	Blocking serum
CD44	1:500	Mouse anti-human	Goat anti-mouse Alexa Fluor 488/568 IgG_{2a}	1:500	10% Goat serum
CD155	1:200	Mouse anti-human	Goat anti-mouse Alexa Fluor 488/568 IgG_1	1:500	10% Goat serum
GFAP	1:200	Rabbit anti-human	Goat anti-rabbit Alexa Fluor 488 IgG	1:500	10% Goat serum

Table 4 gives the details of the primary and secondary antibodies with their respective dilution and blocking serum used for ICC.

2.4.1 Epi-fluorescence microscopy

The slides were viewed using a Zeiss Axiomager Z1 fluorescence microscope equipped with a Hemamatsu digital camera (C4742-95) with GFP/FITC (AF 488-green) and Texas red (AF 568-red) and DAPI (HB-blue) filters to detect fluorescence from labeled cells. Areas of interest were chosen by observing the slides at x10 and then closely examined at x20 & x40 and images were captured using Velocity 4 software (Improvision).

2.5 Total Internal Reflected Fluorescence (TIRF) Microscopy

Specimens were examined with a Zeiss Aviovert 200M incorporating total internal reflected fluorescence (TIRF) microscope which permitted high signal, low noise fluorescence imaging within the tumour cell membrane with great clarity and resolution. Samples were processed as mentioned in section 2.4 however mounting media used had to be of the same refractive index of water. In this case citifluor (Agar Scientific, UK) was used to mount the coverslips onto the slides. Fluorescence was detected using excitation wavelengths of 488nm (green), 568nm (Red) and 405nm (blue) with an argon ion laser. A x100 oil immersion objective with a high numerical aperture objective (NA > 1.3) was used to obtain TIRF images. Images were taken after the correct internal reflectance angle was identified. The TIRF microscope only excites fluorophores which are 50-75 nm from the coverslip and images were captured using the Axiovision software.

2.6 Invasion assay

Invasion assesses the motility of cells and their capacity to adhere to and digest the extracellular matrix in order to invade through. Cell invasion was assessed through the Transwell^{TM} modified Boyden Chamber assay. Cells were grown in serum free media. The Transwell^{TM} inserts used were 8µm porosity, polycarbonate membrane filters within 24-well plates (Corning, UK) and were coated with 50µl (0.5mg/ml) of thawed BD Matrigel^{TM} (Scientific laboratories supplies, UK) then left to dry overnight in the laminar flow hood. The coated inserts were rehydrated the following day with 70µl cold serum free media (SFM) and left for one hour at 37^0C. 10ng/ml platelet-derived growth factor ($PDGF_{AB}$) (Universal Biologicals Cambridge, UK) diluted in SFM was used as a chemoattractant and added to the lower chamber of the well. Cells were harvested, counted and seeded at a concentration of $1x10^5$cells/100 µl SFM in the upper compartment of the transwell unit. Invasion was allowed to occur for 6 hours at 37^0C in a 5% CO_2 chamber. The filters were then removed and fixed with 4% PFA. Non-invading cells on the upper surface of the filter were removed with a cotton swab and invaded cells, adherent on the lower filter surface were characterised through alkaline phosphatase vector red (Vectorlabs, UK) staining. Nuclei were counterstained with Haematoxylin (Dako, UK). Images were captured by a Zeiss Axiophot brightfield microscope using the Axiovision release 4.4 software and cells were counted in 5 random fields. Each experiment was performed in triplicate.

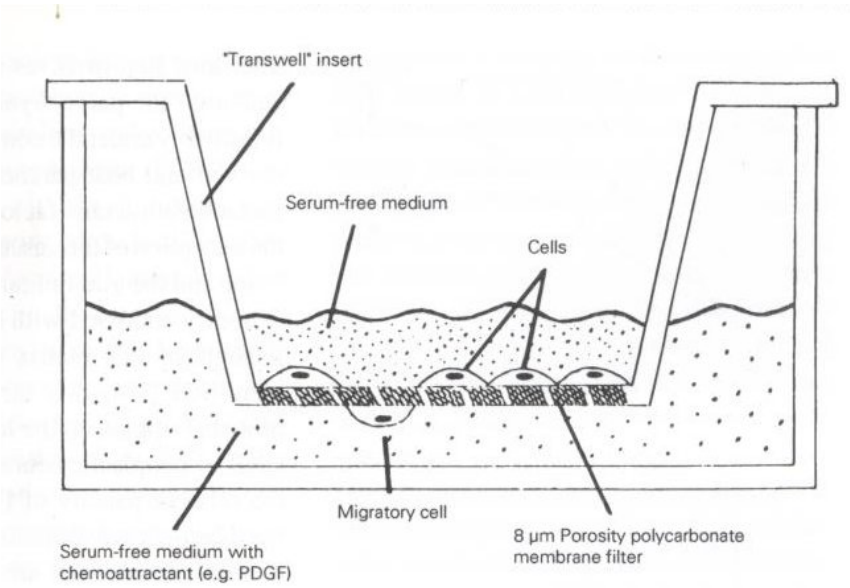

Figure 13: Diagrammatic representation of cross section of a Transwell^{TM} Boyden chamber set-up for an invasion assay (Pilkington, 1996). However, 0.5 mg/ml of matrigel was coated on the membrane filter 24 hours prior the invasion assay.

2.7 Monoclonal Antibody Blocking assay

The monoclonal blocking assay was assessed through the Transwell^{TM} Boyden chamber assay. A normal invasion assay was carried out as explained in section 2.6 however in the upper compartment of the transwell inserts, 100 mg/ml of Monoclonal antibody (Cambridge Biosciences, UK) was added and incubated for 6 hours at 37^0C and 5% CO_2. This step was omitted for the negative control. The positive controls used to validate the blocking antibody specificity were: CD44 (Chemicon, UK) and CD155 (R&D systems, UK). These were commercially available monoclonal antibodies used for ICC and flow cytometry. The filters were then removed and fixed in methanol. Invaded cells on the lower filter surface were stained with Diff Quick (BDH Laboratory Supplies, UK) and

cells were counted in 5 random fields. Each experiment was performed in triplicate. Mean values of invaded cells for each point were calculated. Invasion was expressed as mean ± SEM of the number of total cells counted per well. To note: A time-point analysis (2hr, 4hr, 6hr, 8 hr, 10hr) was carried out before choosing '6 hours' as the optimal incubation time for the blocking assay which was further supported by previous papers (Pilkington *et al*., 1993).

2.7.1 Statistical analysis

Statitistical analysis was performed on the data using one-way ANOVA followed by Tukey's multiple comparison post test with a probability of less than 0.05 being regarded as significant. The software package GraphPad Prism 3.02 was used to calculate the statistical tests where all data are expressed as mean values.

2.8 Transfection of cells with siRNA CD44 and siRNA CD155

The introduction of siRNA for a particular gene is used to evaluate gene knock-down. However the key step for maximum transfection efficiency and minimal cytoxicity is the efficient delivery of nucleic acids to the cells. Accell^{TM} siRNA and reagents (Thermo Scientific Dharmacon, UK) was used to achieve transfection. These siRNAs were specifically modified for use without a transfection reagent and work at a higher concentration than the conventional siRNA with minimal disruption of the expression profile and when used with Accell siRNA delivery media, little or no delivery optimization

was required. The Accell^{TM} siRNA control kit (Thermofisher scientific, UK) was used to test for target specificity, stability and successful uptake of the siRNAs by cells. The controls used were as follows:

Table 5: Positive and negative controls used for validation of transfection studies:

Target gene	Accession number	Description
GAPD	NM_002046	Species-specific control siRNAs designed to silence target genes.

Table 5.1 shows the positive control used to validate the results from the transfection studies. GAPD siRNA was used as a house-keeping gene.

Primer name	Description
Accell non-targeting pool siRNA	Negative control pool of 4 siRNA with at least 4 mismatches to any human, mouse or rat gene. Designed not to target any genes in the human, mouse or rat genomes.

Table 5.2 shows the negative control used as a validation of the transfection studies.

Table 6 RNA sequences of Accell™ siRNA used in the transfection studies

Primer Name: Accell SMARTpool siRNA CD44	Target sequence
A-009999-14, CD44	CUC UGA GCA UCG GAU UUG A
A-009999-15, CD44	CCA UUC ACC UUU AUG UUA U
A-009999-16, CD44	CCU UUG AUC AGU AUA AUU U
A-009999-17, CD44	CUG UUA UAU CAG AGG AGU A

Table 6.1 shows primer name and sequence of each siRNA primer. The primers were supplied as SMARTpool® siRNA (Dharmacon, UK). On receipt of siRNA Duplexes, they were resuspended in 100µl 1 X siRNA buffer to make a 100µM solution as per the manufacturer's guide.

Primer Name: Accell SMARTpool siRNA CD155	Target sequence
A-015323-13, PVR	GGA UCG GGA UUU AUU UCU A
A-015323-14, PVR	CUA UGA UCU UGA GGG CAG A
A-015323-15, PVR	UCU UUG UGU CCA GAG UUU U
A-015323-16, PVR	GGU GCA AGU UCA UAG GUC U

Table 6.2 shows primer name and sequence of each siRNA primer. The primers were supplied as SMARTpool® siRNA (Dharmacon, UK). On receipt of siRNA Duplexes, they were resuspended in 100µl 1 X siRNA buffer to make a 100µM solution as per the manufacturer's guide.

Transfection reagents affect viability of cells, in particular in antibiotic containing media, therefore, 48 hours prior to transfection, media was changed to antibiotic free medium and weaned onto to Accell siRNA delivery media (Dharmacon,, UK) and 3% FCS. Cells were harvested and plated into 96 well plates at an approximate seeding density of $1x10^4$ to achieve 90% confluency at the time of transfection (All amounts and volumes are given on a per well basis for 96 well plate formats and can be scaled up or down for other well formats). 7.5µl of the 100µM siRNA was mixed with 750µl delivery media resulting in a final concentration of 1µM Accell siRNA per well. The growth media was removed from wells and replaced with 100µl of the delivery mix (Accell siRNA and Accell delivery media) per well. Plates were then returned to the incubator for 96-120 hours and gene knock-down was evaluated.

2.9 Western blotting

Cells were washed with PBS before 250µl of the lysis buffer was added to the cells. The lysis buffer was comprised of 1ml of RIPA buffer (Thermofisher, USA) and 10µl Halt™ Protease and Phosphatase Inhibitor cocktail. The flask was transferred immediately on ice and left to incubate for 5 minutes on a plate shaker (Platform Shaker STR6, UK). The cells were scraped off the substrate and the lysate was used for protein quantification which was carried out using the Bradford protein assay (Dako, UK) with a standard curve bovine serum albumin (BSA) concentration curve constructed. Samples were mixed with Laemmli sample buffer (Biorad, UK) with β-mercaptoethanol and 20µg of protein per lane were loaded for 10% acrylamide SDS-PAGE. Proteins were then electrophorectically transferred

to a polyvinylidenefluoride (PVDF) membrane (Biorad, UK) which was then incubated in blocking solution: 0.5-5% dried milk in Tris buffered saline (TBS; 150 mM NaCl, 10 mM Tris pH 7.4) with 0.05% Tween 20. Primary antibody incubation was carried out overnight at 4^0C and secondary antibody horseradish peroxidase-conjugates added at 1:1000 for one hour at room temperature. Extensive washing of the membranes in TBS with 0.05% Tween were carried out after each incubation and immunocomplexes were revealed using an enhanced chemiluminescence reagent (Cheshire sciences, UK) according to the manufacturer's protocol and light sensitive films (Amersham, UK).

2.10 Proliferation assay

Here, the Bromodeoxyuridine (BrdU) cell proliferation assay kit (Chemicon, UK) was used to assess the proliferative rate (S-phase) of the cells under study. As per the manufacturer's guide, two types of control are recommended to insure the viability of the experiments, namely blank (only tissue culture supernatant added to the well) and background (cells were present but no BrdU reagent added to the well). Cells were seeded in a 96 well plate at a density of 2 x 10^5 cell/ml in 100µl/well of appropriate culture media and left to adhere properly for 24 hours at 37^0C/ and 5% CO_2. BrdU was added at least 2 hours (the time mentioned was related to the population doubling time of the cell line under study; refer to section 3.3) prior to the end of the incubation period and pipette 20µl of the diluted BrdU label (1:500 of concentrated stock: culture media) to the appropriate wells and incubate for 16-18 hours. The labeling solution was removed, 200µl/well of the fixing solution was added to the cells and the plate was incubated for 30 minutes at room

temperature. The plate was washed 3 x with washing buffer provided in the kit. 100µl/well of anti-BrdU monoclonal antibody was added to the wells and incubated for 1 hour at room temperature. The plate was then washed 3x with washing buffer and 100µl of goat anti-mouse IgG peroxidase conjugate was added and incubated for 30 minutes at room temperature. The plate was washed again 3x with washing buffer and 100µl/well of tetramethylbenzidine (TMB) peroxidase substrate was added and incubated for 30 minutes at room temperature in the dark. Positive wells were visible by a blue colour, the intensity of which is proportional to the amount of BrdU incorporation in the proliferating cells. The reaction was stopped by pipetting 100µl/well of the acid solution provided into each well where the colour of the positive wells changed from blue to bright yellow. The plate was read using a spectrophotometer microplate reader (POLARstar OPTIMA BMG LABTECH) set at dual wavelength of 450/550nm. The higher the optical density (OD) reading reflected the higher the BrdU concentration in the sample. All tests were done in triplicate and repeated three times to achieve statistical validity.

2.10.1 Statistical analysis

Statitistical analysis was performed on the data using one-way ANOVA followed by Tukey's multiple comparison post test with a probability of less than 0.05 being regarded as significant. The software package GraphPad Prism 3.02 was used to calculate the statistical tests where all data are expressed as mean values.

2.11 Adhesion Assay

The ECM cell adhesion array kit (Chemicon, UK) used provided an ECM array microtiter plate with a homogenous fluorescence detection format allowing quantitative comparison of multiple samples. The ECM Array plate consisted of one 96-well plate with 7 strips consisting of 6 different human, ECM-coated wells (Collagen I, Fibronectin, Laminin, Tenascin, Vitronectin) and one BSA-coated well. Experimental cells at a density of 3 x 10^6 cells/ml were seeded onto each of the substrates named above. The plate was then incubated for 2 hours at 37^0C in a CO_2 incubator. Subsequently, unbound cells were washed away and adherent cells were lysed with 1mol NaOH and detected by the CyQuant GR® dye. This green-fluorescent dye exhibits strong fluorescence enhancement when bound to cellular nucleic acids. Relative cell attachment was determined using a fluorescence plate reader with 485nm and 530nm filter sets. All tests were carried out in triplicate and repeated three times.

2.11.1 Statistical analysis

Statitistical analysis was performed on the data using one-way ANOVA followed by Tukey's multiple comparison post test with a probability of less than 0.05 being regarded as significant. The software package GraphPad Prism 3.02 was used to calculate the statistical tests where all data are expressed as mean values.

2.12 Confocal Microscopy

Confocal images were captured using the x40 (oil immersion) (Numerical aperture 0.5 and 1.3 respectively) objective of a Zeiss meta LSM 510 Axioskop2 confocal microscope. Fluorescence was detected using excitation wavelengths of 488nm (green), 568nm (red) and 405nm (blue), with an argon, HeNe1 and diode laser respectively. Images were taken using optimal settings for pinhole diameter, detector gain and offset acquisition to detect positive immunofluorescence labeling with minimal background. Multi track image capture was used, with two channels so that separate channels could image different colours to help prevent any overlap in excitation spectra. Identical settings were then used to image negative controls in which the primary antibody was omitted.

Table 7 Primary and secondary antibodies used with their corresponding blocking and buffers

Primary Antibody	Dilution	Species	Secondary Antibody	Dilution	Blocking serum
CD44	1:500	Mouse anti-human (Millipore)	Goat anti-mouse Alexa Fluor 488/568 IgG_{2a}	1:500	10% Goat serum
CD155	1:200	Mouse anti-human (R&D systems)	Goat anti-mouse Alexa Fluor 488/568 IgG_1	1:500	10% Goat serum
β_1 integrin	1:100	Rabbit anti-human (Abcam)	Goat anti-rabbit Alexa Fluor 488 IgG	1:500	10% Goat serum
$\alpha_v\beta_1$ integrin	1:200	Mouse anti-human (Abcam)	Goat anti-mouse Alexa Fluor 488 IgG_3	1:500	10% Goat serum
$\alpha_v\beta_3$ integrin	1:250	Mouse anti-human (Abcam)	Goat anti-mouse Alexa Fluor 488 IgG_1	1:500	10% Goat serum
F-Actin-conjugated 488	1:40	Mouse anti-human (Invitrogen)	Goat anti-mouse Alexa Fluor 488 IgG	*'prediluted by supplier'*	10% Goat serum

Table 7.1 gives the details of the primary and secondary antibodies with their respective dilution and blocking serum used for confocal microscopy

To confirm the confocal microscopy results, western blotting was performed on SNB-19 cells (untreated, siRNA CD44-treated and siRNA CD155-treated). (Method has been described in section 2.9)

Primary Antibody	Dilution	Species	Secondary Antibody	Dilution	Molecular weight
F-actin	1:250	Mouse anti-human (Abcam)	HRP goat anti-mouse (Dako)	1:000	43 kDa
α_v integrin	1:250	Mouse anti-human (BD Biosciences)	HRP Goat anti-mouse (Dako)	1:1000	125 kDa
β_1 integrin	1:500	Rabbit anti-human (BD Biosciences)	HRP Goat anti-rabbit (Sigma)	1:1000	88 kDa
β_3 integrin	1:2500	Mouse anti-human (BD Biosciences)	HRP Goat anti-mouse (Dako)	1:1000	104 kDa

Table 7.2 gives the details of the primary and secondary antibodies with their respective dilution and expected molecular weights identified used to confirm the confocal microscopy results.

2.13 Live cell imaging (Real-time Kinetic Microscopy)

Live cell imaging permits cells to be maintained in a healthy state and function normally on the microscope stage. Live cell imaging chambers effectively combine a cell culture incubator with an inverted microscope to provide almost total control of the environment, the incubator enclosure surrounds the microscope stage, objectives, fluorescence filters and transmitted light condenser. Temperature is controlled with an external heating unit and carbon dioxide concentration is controlled with a sensing unit coupled to a regulator that is fed by a cyclinder of pure gas.

Cells of interest were plated at 30% confluency in a 24 well plate and left to adhere overnight prior the experiment. The Zeiss Axiovert 200M live cell (time-lapse) microscope was then set up to image 1 point in each well, once every 30 minutes over 72 hours using the DAPI filter to monitor cells under treatment. The images were collated and a movie sequence generated. Tracking of cells for speed of movement and distance moved were enabled using the Volocity 4 software. 10 cells were tracked randomly for each well and each experiment was done in triplicate and repeated three times.

2.13.1 Statistical analysis

Statitistical analysis was performed on the data using one-way ANOVA followed by Tukey's multiple comparison post test with a probability of less than 0.05 being regarded as significant. The software package GraphPad Prism 3.02 was used to calculate the statistical tests where all data are expressed as mean values.

2.14 Signal Transduction Pathways

The Rho family of small GTPases, including Rho, Rac and cdc42, acts as molecular switches to regulate processes such as cell migration, adhesion, proliferation and differentiation.

The Rho-GTPase Antibody sampler kit (Cell signaling Technology, UK) was used in the scope of this thesis. Cells (under different treatment regimes) were subjected to Western blotting (as described in section 2.9)

Table 8 Primary and secondary antbodies used with their corresponding dilutions

Primary Antibody	Dilution	Species	Secondary Antibody	Dilution	Molecular weight
Cdc42	1:250	Rabbit anti-human	HRP Goat anti-rabbit	1:000	21 kDa
Phospho-Rac/cdc42	1:100	Rabbit anti-human	HRP Goat anti-rabbit	1:1000	28 kDa
Rac 1/2/3	1:500	Rabbit anti-human	HRP Goat anti-rabbit	1:1000	21 kDa
RhoA	1:500	Rabbit anti-human	HRP Goat anti-rabbit	1:1000	21 kDa
RhoB	1:500	Rabbit anti-human	HRP Goat anti-rabbit	1:1000	21 kDa
RhoC	1:500	Rabbit anti-human	HRP Goat anti-rabbit	1:1000	21 kDa

Table 8 gives the details of the primary and secondary antibodies with their respective dilution and expected molecular weights identified used for signal transduction pathways analysis

2.15 Statistical significance

Unless stated otherwise, all experiments were done in triplicate and the appropriate statistical analyses employed to ensure statistical validity.